A WATER-ENERGY NEXUS APPROACH FOR THE CO-OPTIMIZATION OF ELECTRICAL AND WATER SYSTEMS

by

Mennatalla Ahmed Elbalki

A Thesis presented to the Faculty of the
American University of Sharjah
College of Engineering
In Partial Fulfilment
of the Requirements
for the Degree of

Master of Science in
Electrical Engineering

Sharjah, United Arab Emirates

May 2023

Declaration of Authorship

I declare that this thesis is my own work and, to the best of my knowledge and belief, it does not contain material published or written by a third party, except where permission has been obtained and/or appropriately cited through full and accurate referencing.

Signature: Mennatalla Ahmed Elbalki

Date 5/5/2023

Approvals

We, the undersigned, approve the Masters Thesis written by: Mennatalla Elbalki

Thesis Title: A Water-Energy Nexus Approach for the Co-optimization of the

Electrical and Water Systems

Date of Defense: 01/05/2023

Name, Title and Affiliation	**Signature**
Dr. Mostafa Shaaban Associate Professor Department of Electrical Engineering Thesis Advisor	
Dr. Ahmed Osman Professor Department of Electrical Engineering Thesis Co-advisor	
Dr. Shayok Mukhopadhyay Associate Professor Department of Electrical Engineering Thesis Examiner (Internal)	
Dr. Md. Mortula Professor Department of Civil Engineering University Name: American University of Sharjah Thesis Examiner (External)	

Accepted by:

Dr. Fadi Aloul
Dean
College of Engineering

Dr. Mohamed El-Tarhuni
Vice Provost for Research and Graduate Studies Office of
Research and Graduate Studies

Acknowledgments

The guidance and support of many individuals and professionals allowed me to accomplish my research successfully and effectively. First and foremost, I would like to express my special thanks and sincere gratitude to Dr. Mostafa Shaaban and Dr. Ahmed Osman for their time, valuable guidance, continuous assistance, consistent support, and feedback in every phase of the research.

Also, I would like to thank the professors of the Electrical Engineering department for their crucial knowledge, academic support, and advice that encouraged me throughout my master-level courses. Their expertise and encouragement have been invaluable to me. Furthermore, I am deeply grateful for Eng. Ariana Pietrasanta's and Eng. Abdelfatah Ali's assistance and contribution throughout my research stages.

Lastly, I would like to express my deepest appreciation to my family and friends for their love and support, which has been a constant source of motivation and endless inspiration.

Dedication

To my family…

Abstract

Water and electricity are two essential and critical needs for living; however, water scarcity and uncertainty are becoming more prominent. Water networks are energy-demanding industries where a significant amount of electricity is consumed in various water processes. Also, thermal desalination systems are usually a part of a cogeneration process, which cogenerates electricity and freshwater. Therefore, water and electrical networks can't be entirely independent by which a more integrated approach, Water-Energy Nexus (WEN), is developed. A WEN is the basis of a smart city where water and electrical networks are interconnected and integrated by implementing efficient management strategies. Accordingly, this study develops a co-optimization model for the design and operation of the integrated power and water systems. The proposed co-optimization model minimizes the total annual cost of the micro-WEN system while capturing its optimum design values and operating conditions and meeting the electrical and water demands. For a smart grid, three main characteristics are considered to enhance its efficiency and reliability: Integrating distributed energy resources, including renewable resources, grid operations, and resources optimization, and utilizing advanced electricity storage technologies. Improving the efficiency and reliability of a water network can involve a variety of measures: Improving the pump station design, system configuration, and valve distribution, installing variable speed drives (VSDs) for pumps, and including water storage tanks. The design and operational problems are formulated as non-linear programming (NLP) in General Algebraic Modelling System (GAMS) environment. This work presents a plan for the transition from thermal desalination to RO desalination in UAE, where electricity and water production are decoupled to address the problem of operating UAE's power plants during the winter at low efficiency to be able to meet the water demand. The results show that the optimal design of the cogeneration unit has a power generation capacity of 150 MW and a water production capacity of 145 m^3/h to meet the electrical and water demands at a minimum total annual cost. Moreover, the simulation results assert that the co-optimization model provides a reduction in the total operational cost of 1.23% and 26.7% with the integration of PVs and shifting to RO with PV, respectively.

Keywords: NLP; optimization; multi-effect distillation (MED); a combined cycle power plant (CCPP); reverse osmosis (RO); water-energy nexus (WEN).

Table of Contents

List of Figures

List of Tables

List of Abbreviations

AC	Air Compressor
APH	Air Preheater
CC	Combustion Chamber
CCPP	Combined Cycle Power Plant
CHP	Combined Heat and Power
CSP	Concentrated Solar Power
ED	Electrodialysis
GAMS	General Algebraic Modeling System
HESS	Hydrogen Energy Storage System
HRSG	Heat Recovery Steam Generators
MED	Multi-effect Distillation
MSF	Multi-stage Flash
NLP	Non-Linear Programming
PV	Photovoltaics
RO	Reverse Osmosis
WEN	Water Energy Nexus

Nomenclature

A. Sets and Indices

g	Index of generators
i, j	Index of buses of electrical network
k	Index of streams in CCPP
n	Number of distillation effects in MED
t	Index of time periods

B. Parameter

b_g	Fuel cost coefficient of generator g
C_e	Electricity cost, \$/kWh
C_f	Fuel cost, \$/MJ
C_{lab}	Labour cost factor, \$/m^3
$C_{mat,MED}$	Material correction factor for MED
$C_{p,a}$	Specific heat at constant pressure of air
C_{st}	Steam cost, \$/kg
C_{swip}	Seawater intake and pre-treatment cost, \$/m^3/day
CRF	Capital recovery factor
f	Plant availability
K_{MED}	Cost factor, \$/ m^2
K_s	Salt permeability coefficient, m^3/m^2 s kPa
K_w	Water permeability coefficient, m^3/m^2 s kPa
LHV	Lower heating value, kJ/kg
M_f	Molecular weight of fuel

MTF	Maintenance factor
N_{CCPP}	Index of time segments
N_{MED}	Annual operation time, h/yr
n_{RO}	Number of membranes in RO
η_{CC}	First-law efficiency of combustion chamber
$P_{i,t}^{L}$	Active power load of bus i at time t, MW
$P_{i}^{g,\max}$	Maximum limit of active power output of g connected to i
$P_{i}^{g,\min}$	Minimum limit of active power output of g connected to i
$P_{ij}^{\max}$	Maximum limit of active power flow of branch ij
ρ^{b}	average density of vapor formed by boiling, kg/m^3
ρ^{s}	average density of seawater, kg/m^3
$Q_{i,t}^{L}$	Reactive power load of bus i at time t, MW
$Q_{i}^{g,\max}$	Maximum limit of reactive power output of g connected to bus i
$Q_{i}^{g,\min}$	Minimum limit of reactive power output of g connected to bus i
$Q_{ij}^{\max}$	Maximum limit of reactive power flow of branch ij
$scal_{MED}$	Scaling exponent of MED
T_{feed}	Intake seawater temperature, °C
U	Overall heat transfer coefficients, kW/(m^2 °C)
W_{MED}	Consumption of electric power of MED, kWh/m^3
$W_{demand\ (t)}$	Water demand at time t, m^3/hr
X_{O_2}	Molar fraction of oxygen
X_{b}	Salt concentration in brine, ppm
X_{f}	Salt concentration in feed seawater, ppm

Y_a Specific heat ratio of air

Z_{ij} Impedance of branch ij

$\triangle P_{CC}$ Pressure difference in combustion chamber

$\triangle TLM$ Log mean temperature difference

θ_{ij} Phase angle of impedance of branch ij

C. Variables

A_n Heat transfer surface area in effect n, m^2

A_{RO} membrane area, m^2

AOC Annual operational cost

B_n Brine flow rate in effect n of MED, kg/s

h_k Specific enthalpy of stream k, kJ/kg

HTA_{MED} Total heat transfer surface area of MED, m^2

L_s Latent heat of motive steam, kJ/kg

$L_{v\,(n)}$ Latent heat in effect n, kJ/kg

m_a Air mass flow rate, kg/s

m_b Brine mass flow rate in RO, kg/s

m_c Exit water to sea from main condenser, kg/s

m_{dis} Net distillate produced from MED, kg/s

m_f Fuel mass flow rate, kg/s

m_{feed}^{MED} Feed water flow rate at first effect in MED, kg/s

m_{feed}^{RO} Feed water flow rate in RO, kg/s

m_g Combustion gases mass flow rate, kg/s

m_p Permeate mass flow rate, kg/s

m_s	Steam mass flow rate, kg/s
m_{salt}	Salt mass flow rate, kg/s
m_{sea}	Seawater mass flow rate, kg/s
η_{AC}	Compressor isentropic efficiency
η_{GT}	Gas turbine isentropic efficiency
η_{ST}	Steam turbine isentropic efficiency
η_{RO}	RO efficiency
p_e	Forecasted electricity price at power transmission bus, $/kWh
$P_{i,t}^{g}$	Active power generation of bus i at time t, MW
$P_{ij,t}$	Active power flow of branch connecting bus i to j at time t, MW
P_k	Pressure of stream k, bar
$P_{h,f}$	Feed hydraulic pressure, kPa
$P_{h,b}$	Brine hydraulic pressure, kPa
$P_{h,p}$	Permeate hydraulic pressure, kPa
$Q_{i,t}^{g}$	Reactive power generation of bus i at time t, MW
$Q_{ij,t}$	Reactive power flow of branch connecting bus i to j at time t, MW
SR	Salt rejection
$T_{MED\ (n)}$	Temperature profile in effect n, °C
T_{cfeed}	Seawater temperature leaving main condenser, °C
T_{cond}	Temperature profile in main condenser, °C
T_k	Temperature of stream k, K
T_s	Temperature of motive steam, °C
TAC	Total annual cost

TCC	Total centralized cost
$V_{i,t}$	Voltage magnitude of bus i at time t, V
V_n	Vapor flow rate in effect n, kg/s
V_s	Motive steam flow rate, kg/s
W_{AC}	Consumption of power of air compressor, MW
W_{GT}	Generation of power of gas turbine, MW
W_{ST}	Generation of power of steam turbine, MW
W_{net}	Total generation of power of CCPP, MW
$W_{res\,(t)}$	Reservoir capacity at time t, m^3/hr
W_{RO}	Power consumption of RO, kWh
X_{avg}	Average salinity on feed side, kg/m^3
X_{last}	Salt concentration in rejected brine, ppm
X_p	Salt concentration in permeate, ppm
π_f	Feed osmotic pressure, kPa
π_b	Brine osmotic pressure, kPa
π_p	Permeate osmotic pressure, kPa
$\delta_{i,t}$	Voltage angle of bus i at time t, rad

Chapter 1. Introduction

This chapter concisely introduces the water and energy interrelationship, competition and conflicts between water and energy, and challenges, opportunities, and themes of the water-energy nexus. Also, it gives a brief overview of desalination technologies and cogeneration plants. Then, it addresses the objectives and the contributions of the thesis. Lastly, the organization of the thesis is outlined.

1.1. Overview

Water is one of the most crucial and essential human survival resources. There are no substitutes for water, and it should be reutilized. However, various issues like growing population, climate change, industrialization, technology, and food production potentially lead to water scarcity, uncertainty, and variability [1]. According to the food and agricultural organization's (FAO) AQUASTAT, global water use is roughly calculated to be 70% of the world's total available freshwater supply by 2050 [2]. Also, energy is fundamental and vital for a satisfactory and decent life. Clean energy and freshwater are required to ensure society's sustainable, environmental, social, and economic development. Thus, water and energy networks are developed and managed to provide the basic resources and services to communities, ensuring security and reliability.

The water-energy nexus refers to the complex interdependence between the availability of water resources and the generation and use of energy [3]. Considering a smaller scale, micro water-energy nexus incorporates a microgrid where an electrical network with a local supply source operates independently and acts as a single entity. This relationship has become increasingly important as the world faces challenges such as population growth, urbanization, and climate change, which are putting pressure on both water and energy systems [4]. As the world's population is projected to increase by 2 billion people by 2050, leading to an increased demand for water and energy, approximately 40% of the world's population is anticipated to suffer from the issue of water scarcity. Consequently, water and power operations and systems must be planned simultaneously together. The integration of thermal desalination of seawater in the combined cycle power generation plant by utilizing the steam discharged from steam generators has been indicated as a promised enhancement in power generation and water desalination. Although, developing advanced resource management is necessary to minimize the

operational cost of the micro-WEN system and optimize the utilization of energy resources fed to the power plant.

There are several strategic aspects that provide essential support for the water-energy nexus (WEN); for instance, optimizing the freshwater efficiency of energy production and electricity generation, optimizing the energy efficiency in managing, distributing, and treating water, and improving water and energy networks' reliability and resilience [1].

One theme that emerges is the potential for renewable energy sources to reduce the demand for water in the energy sector [5]. For example, hydropower is a renewable energy source that relies on the availability of water resources, and the use of hydropower can significantly reduce the demand for water in the energy sector compared to the use of fossil fuels [6]. Similarly, using solar photovoltaics (PV) and wind power can also reduce the demand for water in the energy sector, as these technologies do not require water for cooling or other purposes [7].

Another theme is the potential for water resources to be used for the generation of electricity. For instance, the use of seawater reverse osmosis (RO) for desalination can be powered by renewable energy sources such as solar PV, reducing the carbon footprint of both water and energy production [8]. In addition, the use of osmotic power, also known as blue energy, can harness the energy potential of the natural osmotic pressure gradient between freshwater and seawater to generate electricity [9].

A third theme is the potential for integrated water and energy systems to improve the sustainability of both sectors. Accordingly, using wastewater treatment plants to generate energy through processes such as anaerobic digestion or microbial fuel cells can help reduce the demand for fresh water while also producing clean energy [10]. Similarly, the integration of water and energy systems through the use of smart grids can enable the optimization of energy production and water management, improving the overall efficiency and sustainability of both systems [11].

Thermal desalination and RO are the two leading desalination technologies. Thermal desalination has two primary types: multi-effect distillation (MED) and multi-stage flash (MSF) distillation, which are conventionally a part of a combined cycle or a cogeneration power plant. In thermal desalination plants, to separate the dissolved

minerals, the water is evaporated and cooled afterward. Compared to RO desalination plants, thermal desalination plants don't clog filters or membrane; moreover, it consumes less electricity and produces less waste. For the operation of a MED plant, at its first effect, low temperature steam is mainly required to evaporate the water that passes through its series evaporators [12].

Cogeneration is a system that utilizes one primary energy source to produce two or more useful forms of energy at once. For example, in a combined cycle gas turbine (CCGT), a gas turbine converts mechanical energy into electricity and exhausts waste heat, which a steam turbine uses to generate additional electricity. The steam turbine produces electric energy and supplies a tremendous amount of low-pressure steam [13]. As thermal energy is an essential energy input to produce freshwater, desalination processes like MED and MSF and power generation are integrated on the same site with the aim of satisfying demand from both sectors, water and energy, respectively.

1.2. Thesis Objectives

This thesis mainly aims to develop a new co-optimization and a co-operation mathematical model for a generation-level micro water-energy nexus network. Most importantly, the proposed co-optimization model quantifies the mass and energy streams of the cogeneration power plant, considering several plant variations. The proposed system can tackle different objectives, but mainly minimizing the operational cost and meeting the electrical and water demands will be the priority. Several case studies are performed to validate the effectiveness of co-operating and co-optimizing the two systems simultaneously.

1.3. Research Contribution

The contribution of this research work can be summarized as proposing a new co-optimization framework for the design and operation of a micro-WEN system that meets loads of the electrical and water networks at a minimum cost.

1.4. Thesis Organization

The rest of the thesis is organized as follows: Chapter 2 reviews and analyses work related to modeling the integration and co-optimization of electrical and water networks. Chapter 3 introduces the proposed models to formulate the proposed micro-WEN system and discusses the solving approach. Case studies and their simulation

results are presented and discussed in Chapter 4. Finally, Chapter 5 infers the thesis's conclusion and outlines a plan for possible future works.

Chapter 2. Background and Literature Review

In this chapter, a baseline of knowledge about WEN and definitions of its structure components are discussed. In addition, various technologies for desalination and renewable energy in the nexus are explored and explained. Then, this chapter addresses and investigates several water-energy nexus concepts in the literature for modeling the integration and co-optimization of electrical and water networks.

2.1. Background

The term water-energy nexus (WEN) describes the interdependence of water and energy systems. This interdependence has become significantly crucial as the world's population and economy continue to expand, placing stress on the planet's finite resources and escalating already-existing problems with both. The water-energy nexus is being impacted by climate change, which is changing precipitation patterns and increasing the frequency of extreme weather events that can damage water and energy infrastructure. Considering the water-energy nexus in decision-making and developing integrated water and energy management strategies to address these challenges is crucial. This entails investigating ways to optimize water use in energy production, enhancing the energy efficiency of water infrastructure, and creating integrated water and energy management techniques that can help guarantee a sustainable and resilient water-energy system for the future [1]–[4].

Figure 2-1 provides a graphical illustration of the WEN concept with an integrated power and water utility [14]. This integrated power and water system comprises a power generation consisting of thermal, solar, hydro, and wind power plants, and other renewable energy sources designed to generate electricity for the power grid. Most importantly, these power plants may also include water recovery or recycling systems or use heat from the power generation process to provide energy for desalination. On the contrary, the WEN system consists of a water desalination plant that is utilized to desalinate the water source, seawater, to provide potable water to the water grid. The coproduction plant could be either a thermal desalination or a hydroelectric. Furthermore, a micro-WEN system often includes energy storage technologies, such as batteries, to help ensure a stable and reliable power supply. Optimizing water use and distribution, the WEN uses infrastructure and smart water management systems like

reservoirs, pipelines, and pumps to store and distribute the treated water. To integrate both grids, their production cost functions and the constraints that model their processes are coupled [14].

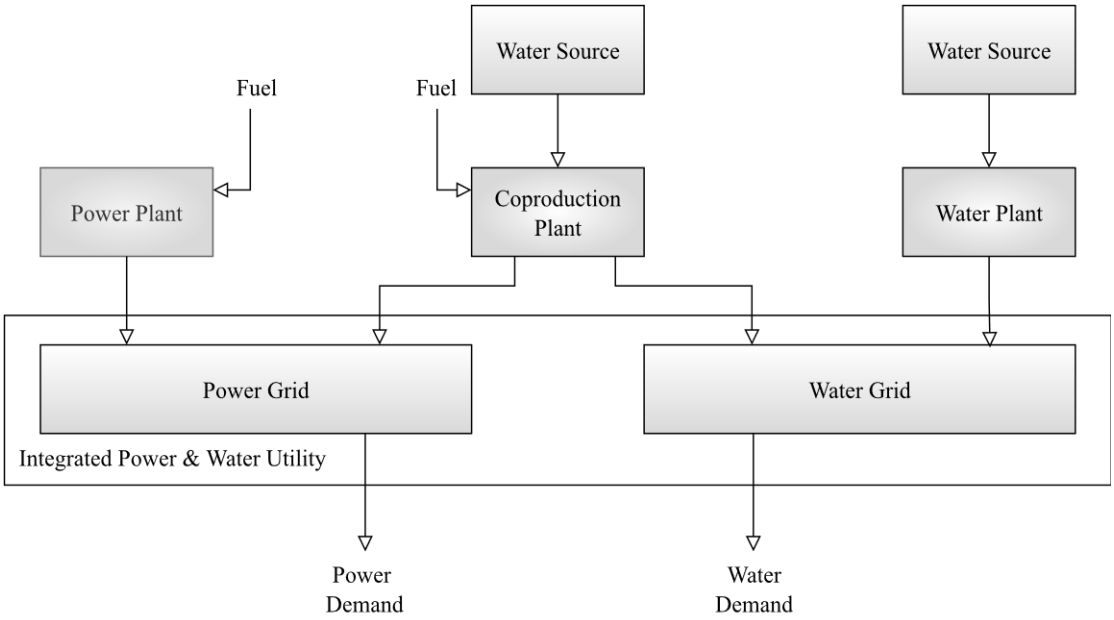

Figure 2-1: Schematic Diagram of a typical micro-WEN [14].

2.1.1. Desalination technologies

Salt and other minerals must be removed to make seawater suitable for irrigation and drinking. Desalination is the term for this procedure. Although desalination technologies have been used for many years, their importance has recently increased as fresh water supplies have been scarce in many regions. Thermal and membrane desalination are the two primary categories of desalination technology. The process is selected depending on variables such as water quality, location, energy intensity, capital costs, and operation and maintenance requirements [12], [15].

Thermal desalination involves heating the seawater to produce steam which is then condensed to produce fresh water. The process is based on the fact that the salt and other minerals in seawater have a higher boiling point than water, so when seawater is heated, the water vaporizes, leaving the salt and minerals behind. The ability of thermal desalination to generate significant amounts of fresh water is one of its key benefits. Additionally, it permits a wide variety of feedwater quality, supporting a range of salinity, temperature, and even some suspended particles. However, the drawback is that it consumes much energy to produce steam and operate the distillation process.

Thus, this can increase the cost of fresh water and make it less economical and more susceptible to changes in energy prices. Multi-stage flash distillation (MSF), a popular technique for thermal desalination, involves rapidly heating and cooling seawater in several stages to produce fresh. Due to the abundance of oil and natural gas resources that supply the energy needed to operate the desalination facilities, MSF desalination is commonly and widely utilized in the Middle East, especially in Gulf countries. However, it is less prevalent in areas where alternative energy sources are available and other desalination types are frequently used. Since thermal desalination also has the disadvantage of emitting enormous amounts of greenhouse gases and other pollutants contributing to water and air pollution, some plants are now utilizing renewable energy sources like solar thermal energy to heat the seawater. Compared to traditional single-effect distillation, multi-effect distillation (MED) minimizes energy consumption and enhances the efficiency of the plant by using the heat of vaporization of water in one effect to heat the seawater in the subsequent effect. The process consists of condensers and evaporators in series where, in the first effect, the seawater is heated and vaporized into steam which is used to heat the seawater in the next effect. Consequently, this cascading process results in a reduction of 50% in the overall energy consumption, resulting in high thermal efficiency. Yet, MED has significant disadvantages; mainly, it is typically a large and complex plant which increases the capital cost and the maintenance requirements [5], [12], [15]–[17].

Alternatively, membrane desalination involves pushing seawater through a semipermeable membrane by which the pressure pushes the smallest molecules in the seawater through the membrane and leaves the larger ones. The most widely used membrane desalination technology is reverse osmosis (RO), a highly efficient and cost-effective desalination method. Reverse osmosis systems typically consist of several components, including a high-pressure pump to pressurize the seawater, a pre-treatment system to remove particles and other impurities that can clog the membrane, and a post-treatment system to remove any remaining dissolved gases and disinfect the water [18]. Some of the main advantages of RO include its high water recovery rate of up to 50% and a high salt rejection rate of over 99% [19]. However, high maintenance costs caused by the regular requirement to replace and clean the membrane is a certain drawback to employing reverse osmosis. Furthermore, RO systems are relatively expensive, particularly when large-scale plants are considered [5], [15]. Another membrane

process is electrodialysis (ED), which utilizes electrical force to allow the salt to pass through the membrane, keeping fresh water behind. Currently, ED is more frequently employed to desalinate brackish water than seawater [15].

2.1.2. Cogeneration plants

Cogeneration plants, commonly referred to as combined heat and power (CHP) plants, are power generation plants that produce electricity and heat simultaneously from a single fuel source. Although CHP facilities have been in use for more than a century, there has recently been a resurgence of interest in them as a way to improve energy efficiency and lower greenhouse gas emissions.

Cogeneration plants have various configurations, including natural gas-fired, biomass-fired, and waste heat recovery systems. The most prevalent type of CHP plant uses natural gas as fuel and is frequently employed in industrial and commercial applications. Nevertheless, biomass-fired cogeneration plants utilize renewable biomass as a fuel source and can be applied to various uses, such as district heating systems. As the name implies, a waste heat recovery system recovers waste heat from industrial processes to produce energy [20].

Cogeneration plants provide better energy efficiency, lower greenhouse gas emissions, and cost savings than conventional power generation systems. By utilizing the waste heat from electricity production for heating and cooling, cogeneration plants can increase overall energy efficiency, significantly reducing greenhouse gas emissions. Moreover, the cogeneration facilities reduce energy costs by eliminating the need for separate power and heating systems and by minimizing the amount of electricity purchased from the grid [21].

To improve the plant's overall energy efficiency and output, the cogeneration plant uses both steam and gas turbines, known as a combined cycle cogeneration plant. This type of cogeneration plant turns the heat from the gas turbine's exhaust into steam which powers a steam turbine to produce more electricity. A vital component of a combined cycle power plant is the heat recovery steam generator (HRSG). Its function is to convert as much gas turbine's exhaust as possible into steam for a steam turbine. Although HRSG designs come in a variety, they all share several common features. Mainly, for water heating, an economizer is the first module that employs low heat to

heat the feedwater. Then, the evaporator heats the hot water to its boiling point. Water and steam are separated in a steam drum at the top of the evaporator. While steam is gathered and transported to the third module, the superheater, the water is recirculated through the evaporator. Finally, before being piped to the steam turbine, the superheater dries the steam and elevates its temperature over the boiling point [22].

Most importantly, the CHP plant's waste heat, exhaust steam, and generated electricity are widely utilized to provide energy for thermal desalination systems, significantly lowering the cost of freshwater produced via desalination. The power and desalination system's production load will fluctuate significantly to satisfy the water and electricity demand, mainly if the power and desalination system operates independently since the water and electricity demand load changes over time. However, integrating and optimizing power and desalination plants can effectively alleviate this issue [23].

2.1.3. Renewable energy

Over the past ten years, the deployment of renewable energy has dramatically increased. This deployment will increase for two main reasons; firstly, more nations realize the advantages of utilizing renewable energy for improved socioeconomic development, increased energy security, and climate change mitigation. Secondly, there is a growing agreement that any global response to catastrophic climate change will necessitate a significant expansion of renewable energy deployment [5]. Most importantly, most challenges of managing WEN can be addressed with the practical applications of renewable energy technologies. Enhancing water security and easing the WEN can be accomplished through the use of renewable energy along various water supply chain segments. For instance, within a conventional water supply chain, as water pumping consumes a significant amount of energy, solar-based pumping solutions are implemented to provide a cost-effective option to pump groups that operate using grid electricity or diesel [24].

The most energy-consuming technology for producing water currently in use is desalination. According to the United Nations-Water Annual Report, desalination technologies utilize at least 75.2 TWh of electricity annually or roughly 0.4% of the total amount used worldwide [25]. Also, IRENA and IEA-ETSAP state that less than 1% of the required energy for desalination plants is currently based on renewables, with the majority from fossil fuels [26]. Since the main desalination technologies are

membrane-based processes that only require electricity or thermal processes that use thermal power or electricity as an energy input, deploying renewable energy provides the chance to separate the supply of fossil fuels from the production of water. There are various methods by that renewable energy can provide thermal or electrical inputs, depending on the desalination technology. Figure 2-2 shows possible configurations of integrating renewable energy technologies like solar and wind resources with various desalination processes. The type and capacity of needed renewable energy for desalination vary by technology. Thus, specific combinations of renewable energy and desalination technologies have arisen, for example, concentrated solar power (CSP) with MED and photovoltaic (PV) or wind with RO. Integrating CSP plants with membrane and thermal desalination technologies is possible because they are built to absorb solar radiation and provide high temperature heat for electricity generation. Moreover, to handle the various load profiles of water and electrical demand without impacting the cogeneration plants' efficiency, CSP plants can be supplied with thermal storage systems. DLR reports that simultaneous electricity and fresh water generation has tremendous potential when using CSP with thermal energy storage in the MENA region, representing around 16% of total water production in 2023 and 22% in 2050 [5].

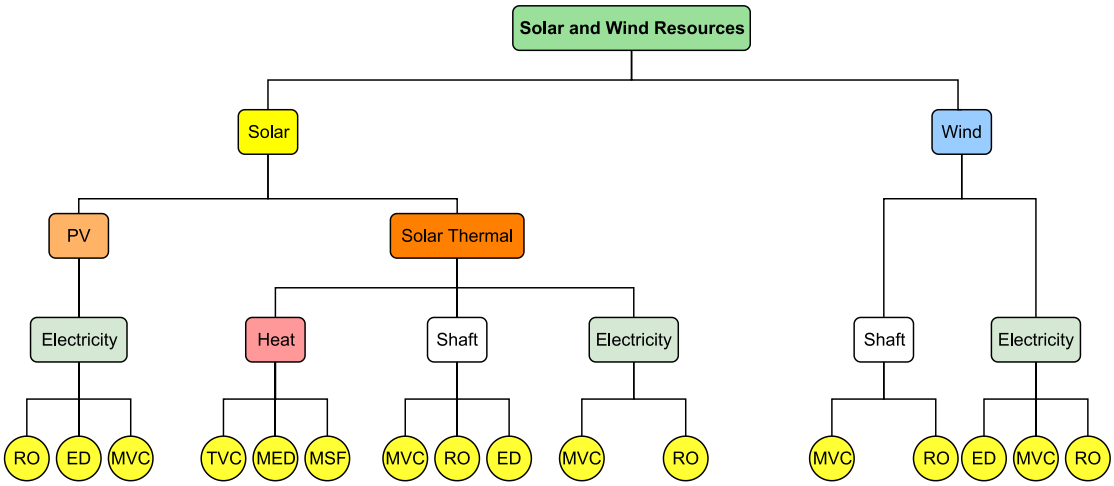

Figure 2-2: Integration of solar and wind resources with desalination technologies [5].

2.2. Related Work

Several water-energy nexus concepts have been investigated in the literature to model the integration and co-optimization of electrical and water networks. The authors, in [27], use Bender's decomposition method to model a robust two-stage operation that

manages the water-energy nexus system at the distribution level with the aim of reducing the operational cost. However, the work assumes that the electrical, gas, and water networks are owned by a single entity. An optimization model is designed for an integrated water and energy supply system for a remote island without access to the utility networks to fulfill the electric and water demands with three different desalination technologies, including MED, MSF, and RO [28]. In [29], a new optimization model is proposed to minimize the operational costs of an integrated water-energy nexus system where wind turbines generate power, and RO desalinates water. This work simplifies the mixed-integer non-linear programming (MNLP) model and utilizes General Algebraic Mathematical Software (GAMS) to attain results with greater accuracy. Considering the uncertainty developed from wind generation outputs, the work in [30] proposes a robust operation model for the multi-energy WEN in which the energy system involves a natural gas transmission, a district heating, a power transmission network, and a water distribution network (WDN).

Also, in [31], Moazeni and Khazaei develop a co-optimization MNLP model by combining the wastewater treatment plant's demand response and the residential loads in the smart grid's economic dispatch. The proposed model minimizes the amount of energy consumed by the wastewater treatment plant and the cost of the power generated at the smart grid and results in high-quality treated wastewater. In [32], the authors introduce the integration of water desalination within security constrained unit commitment (SCUC), which significantly minimizes the systems' operational cost, especially with enormous desalination size.

As the water-energy nexus concept is mainly applied at the supply side, in [33], the work considers the interconnections between water and energy demands in a reservoir to propose new supply-side management of optimal and smart hydro reservoirs. In [33], Charmchi, Ifaei, and Yoo use advanced neural networks to predict two different scenarios that simulate the annual operation and remote monitoring situations.

Nevertheless, several water- energy nexus approaches were investigated on the demand side; for instance, the researchers, in [34], emphasize the pump scheduling and optimizing energy and water flow. In this work, Fooladivanda and Taylor propose a mixed-integer second-order cone programming (MI-SOCP) relaxation to handle the non-convex terms produced by the pumps and pipes' hydraulic characteristics.

Similarly, Mkireb et al. use mixed integer linear to model variable speed pumps with the goal of enhancing the demand response [35].

However, it is noted that the authors, in [36] and [37], discuss the water distribution system's schedule and operation without considering the coordination with electrical systems. Mkireb et al., in [35], present a robust optimization model that manages the uncertainties of the water demand. Atia and Fthenakis introduce active-salinity-control RO to enhance the integration of renewable energy and desalination load, but they don't take into account the demand response uncertainties [36].

To minimize the sum operational cost and to serve the extra wind power systems, using MI-SOCP, the authors, in [38], develop a model that integrates electrical, heating, and water. Likewise, a model that optimally schedules water tanks and pumps is developed in [39] to collect renewable energy from the electrical grid. The proposed model in [40] optimizes the participation of RO desalination in the energy demand response and regulation markets, yet it ignores the constraints of the electrical system. A method that modifies the electric grid economic dispatch is proposed to include a water system by focusing mainly on the cogeneration of electricity and water from fossil fuel plants; however, this work ignores the network structure and other cooperation aspects [14]. Proposed models in [38]–[40] investigate the potential of demand response of the water network as an electric demand, yet the water production isn't linked to the electrical system. The researchers, in [41], use a robust optimization technique (ROT) to model water and electrical demands' uncertainties for a WEN system that mainly consists of combined water-power (CWP) and single water and power energy resources. In [42], the multi-period optimization formulation includes optimal WEN in an integrated power generation and desalination systems' design and operational strategies while considering seasonal variations in water and electrical demands and fuel availability and prices. Deploying renewable energy technologies, the authors, in [43], incorporated solar collectors and batteries to the same WEN's model introduced in [42] with the aim of reducing the carbon footprint.

A novel optimization model is introduced for a water energy nexus-based CHP operation to investigate the relationship between system operation optimization and water conservation [44]. Similarly, a scheduling model is proposed for the optimal

operation of a combined power and desalination (CPD) system, considering MSF, RO, thermal power plants, and water storage simultaneously [45].

Based on the aforementioned discussion, it is clear that the WEN systems aren't modeled with details that allow capturing the integrated system's design and operational variables. Moreover, most of the research works focus deeply on the electric aspect of the system and include minor details about the water network and the desalination processes. On the contrary, research works that deeply tackle various desalination processes don't link water production to the electric system. Most importantly, it is noted clearly that publications that cover mainly the cogeneration of electricity and water from thermal power plants ignore the network structure and other integration aspects. Also, these publications didn't respect the flow limitations and the effort variables, such as pressure and voltage at network nodes. This work builds explicitly upon previous related works to address these aspects and considerations.

Chapter 3. Problem Formulation

The schematic diagram of the proposed micro-WEN is shown in Figure 3-1. The electricity side is a generation network integrated with renewable energy. The combined cycle power plant (CCPP) generates electricity and supplies steam to the MED with the aim of producing freshwater. The water side consists of a thermal desalination system, MED, a RO desalination plant, and a reservoir. Typically, the water network is composed of a pipe network, pumps, and tanks; however, these elements aren't considered in this study for the purpose of simplification. Also, this applies to the storage system. It is crucial to develop a more detailed mathematical model of the micro-WEN system to operate the presented micro-WEN, considering more variables and more complex interactions between system components.

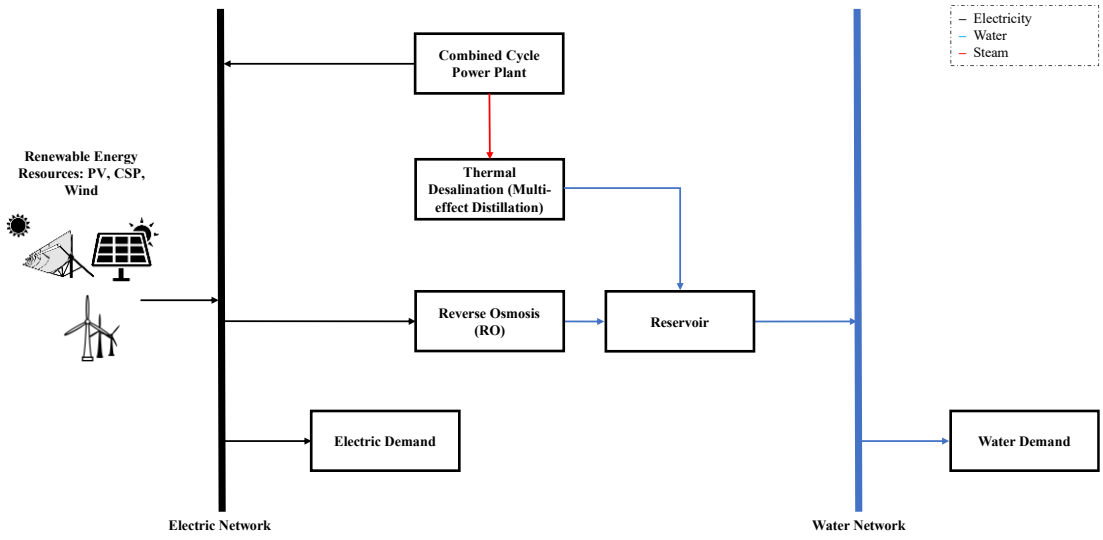

Figure 3-1: Physical structure of the proposed micro-WEN.

This chapter is dedicated to representing the formulation of the problem. A basic electrical network is modeled, and the IEEE 24-bus test system is selected as the test model for the power generation system. Before proceeding to the mathematical model formulations of CCPP, MED, and RO, some prerequisite assumptions and simplifications are highlighted to facilitate the modeling. Also, a mathematical model is proposed for a basic water network comprising a reservoir that fulfills a specific daily water demand. Then, some constraints of power injection and mass flow rate and temperature of steam act as the connection points of the power and water systems, so

the micro-WEN is integrated. Lastly, economic models used to evaluate the total annual costs of the micro-WEN are presented.

3.1. Mathematical Model of Electrical Network

In this subsection, a basic model of a power generation system is introduced. As shown in Figure 3-2, the test system for the electrical network is selected as IEEE 24-bus test system [46]. This model considers several system constraints as follows:

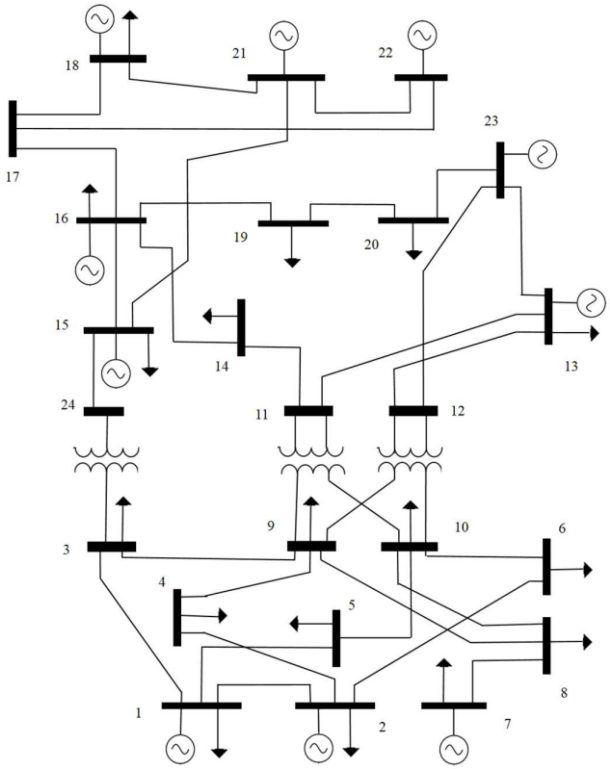

Figure 3-2: IEEE 24-bus system [46].

3.1.1. Power Flow Constraints

These constraints relate the active and reactive power flows in the lines to the voltages and the line impedance as in (1) and (2). Also, the power flow is limited between a minimum and a maximum as in (3) and (4).

$$P_{ij,t} = \frac{1}{Z_{i,j}} \left(V_{i,t}^2 \cos(\theta_{ij}) - V_{i,t}V_{j,t} \cos(\delta_{i,t} - \delta_{j,t} + \theta_{ij})\right) \quad (1)$$

$$Q_{ij,t} = \frac{1}{Z_{i,j}} \left(V_{i,t}^2 \sin(\theta_{ij}) - V_{i,t}V_{j,t} \sin(\delta_{i,t} - \delta_{j,t} + \theta_{ij})\right) - \frac{bV_{i,t}^2}{2} \quad (2)$$

$$-P_{ij}^{max} \leq P_{ij,t} \leq P_{ij}^{max} \quad (3)$$

$$-Q_{ij}^{max} \leq Q_{ij,t} \leq Q_{ij}^{max} \quad (4)$$

3.1.2. Power Balance Constraints

Constraint (5) illustrates the active power balance at each bus in which the right side is the total active power flow from bus i, and the left side reflects the active power generated by the generator g to bus i minus the active power demand at bus i. Similarly, the reactive power balance at each bus is described by (6).

$$P_{i,t}^{g} - P_{i,t}^{L} = \sum_{j \epsilon \Omega^{i}} P_{ij,t} \quad (5)$$

$$Q_{i,t}^{g} - Q_{i,t}^{L} = \sum_{j \epsilon \Omega^{i}} Q_{ij,t} \quad (6)$$

3.1.3. System Constraints

Several variables must be constrained within a reasonable range to ensure the stable and secure operation of the power generation system. Firstly, the voltage's magnitude and angle of each bus are constrained within a suitable voltage level, as shown in (7) and (8), while (9) and (10) fix the voltage's magnitude and angle of the slack bus. Also, (11) and (12) set the maximum and minimum limits of power and reactive generation of generator g connected to bus i.

$$0.9 \leq V_{i,t} \leq 1.1 \quad (7)$$

$$-\frac{\pi}{2} \leq \delta_{i,t} \leq \frac{\pi}{2} \quad (8)$$

$$V_{slack,t} = 1 \quad (9)$$

$$\delta_{slack,t} = 0 \quad (10)$$

$$P_{i}^{g,min} \leq P_{i,t}^{g} \leq P_{i}^{g,max} \quad (11)$$

$$Q_{i}^{g,min} \leq Q_{i,t}^{g} \leq Q_{i}^{g,max} \quad (12)$$

3.2. Mathematical Model of CCPP and MED

In this subsection, a discussion on CCPP and MED modeling is carried. The schematic diagram of an integrated system consisting of a gas turbine, an air preheater (APH), a single pressure HRSG, a steam turbine, and a MED is illustrated in Figure 3-3.

3.2.1. Assumptions and Simplifications

For the modeling of the CCPP, some key assumptions are taken into consideration to simplify its mathematical model. Firstly, the CCPP's fuel is methane (CH_4), and all streams are operating at a steady state. Also, air and combustion gases are considered as ideal gases with constant specific heats [47].

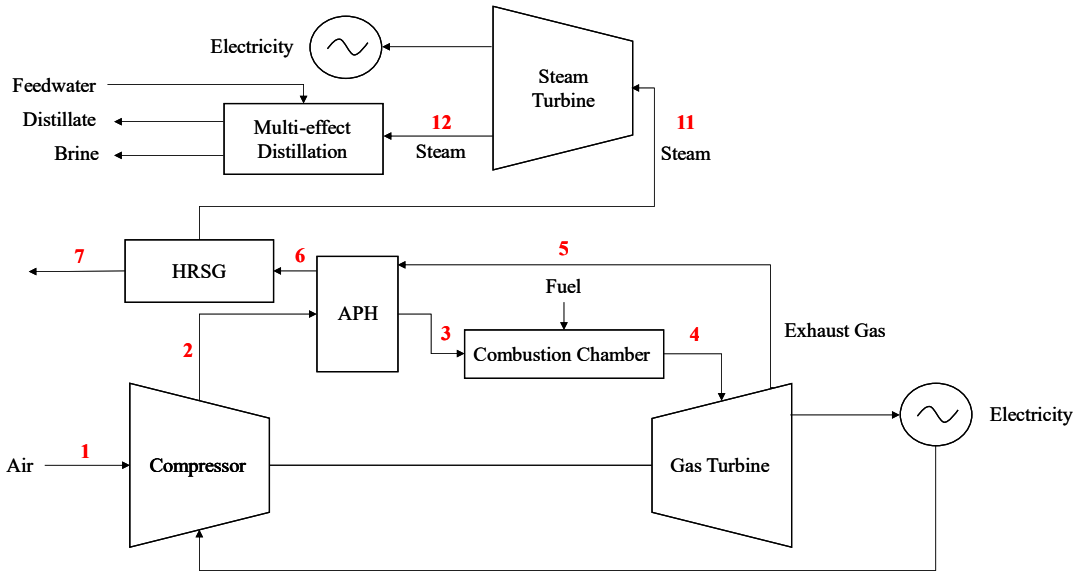

Figure 3-3: Schematic diagram of CCPP integrated with MED.

For modeling the MED system, a few main assumptions are considered to derive its simplified mathematical model. The considered MED configuration is forward feed for simplification, yet the parallel/cross feed is the most energy-efficient feed configuration [48]. For this research, the MED system consists of six evaporators and a main condenser. The non-equilibrium allowance (NEA) is neglected, and the heat transfer area is constant in all effects, as presented in (13). Moreover, the temperature of the sea water is at the saturation temperature of the first effect. At different temperatures and concentrations, the sea water specific heat doesn't change [49], [50].

$$A_{n-1} = A_n \tag{13}$$

For modeling the RO desalination plant, the model considers steady state and isothermal operation. Moreover, compared with the flow rate of the permeate, the salt flow rate across the membrane is neglected. The permeability coefficients of salt and water remain unchanged at different temperatures and concentrations.

3.2.2. Mathematical Model of CCPP

The mass and energy balance equations from stream 1 and stream 6 for various components of the CCPP including air compressor, combustion chamber, gas turbine, and APH are described [47], [51]. First, the air compressor (AC) is modeled using energy equations that are represented in (15) and (16) where Υ_a, specific heat ratio of air, is 1.4, and $C_{p,a}$, specific heat at constant pressure of air, is $1.004\ \mathrm{kJ/kgK}$. Accordingly, (15) models the compression process in the AC, considering the effects of compression efficiency and temperature rise, and (16) relates the power utilized by an AC, W_{AC}, to the mass flow rate of air passing through the compressor, m_a, $C_{p,a}$, and the temperature difference between the inlet and outlet of the compressor.

$$T_2 = T_1\left(1 + \frac{1}{\eta_{AC}}\left[\left(\frac{P_2}{P_1}\right)^{\frac{\Upsilon_a - 1}{\Upsilon_a}} - 1\right]\right) \tag{15}$$

$$W_{AC} = m_a\, C_{p,a}(T_2 - T_1) \tag{16}$$

Mass and energy balance equations for the combustion chamber (CC) are demonstrated in (17), (18), and (19) where LHV, lower heating value f methane, is $50{,}000\ kJ/kg$. Equation (17) represents the conservation of mass principle to ensure that the mass of the gases entering and exiting the system remains constant. In (18), $m_f LHV(1 - \eta_{CC})$ represents the energy lost due to incomplete combustion in the CC, where some fuel doesn't entirely burn and instead exits the system as unburned fuel. The pressure drop across the CC and the amount of energy lost are estimated using (19), which is caused by the resistance of the CC to the flow of gasses. The mass flow rate of the air, m_a, is further expanded in (20) and (21) to illustrate the combustion reaction with molecular weights of fuel, M_f, and air, M_a.

$$m_g = m_a + m_f \tag{17}$$

$$m_a h_3 + m_f LHV = m_g h_4 + m_f LHV(1 - \eta_{CC}) \tag{18}$$

$$P_4 = P_3(1 - \triangle P_{CC}) \tag{19}$$

$$m_a = m_{a,rx} + m_{a,ex} \tag{20}$$

$$\frac{m_f}{M_f} = 0.5\ \frac{X_{O_2}}{M_a}\ m_{a,rx} \tag{21}$$

Mass and energy balances for the APH are identified by (22), (23), and (24) where $C_{p,g}$, specific heat at a constant pressure of a gas, is $1.17\ kJ/kgK$. Equation (22) balances the amount of energy transferred from the air to the gases in the gas turbine.

$$m_a\ C_{p,a}(T_3 - T_2) = m_g\ C_{p,g}(T_5 - T_6) \tag{22}$$

$$P_3 = P_2(1 - \triangle\ P_{a,APH}) \tag{23}$$

$$P_4 = P_3(1 - \triangle\ P_{g,APH}) \tag{24}$$

Equations (25) and (26) model the gas turbine, which generates a net power, W_{net} after subtracting the power used to operate the AC, as shown in (27). Y_g is the specific heat ratio of gas with a value of 1.33 which is utilized to calculate the adiabatic temperature drop that would occur if the expansion in the gas turbine was isentropic. Accordingly, (25) calculates the temperature drop across the gas turbine.

$$T_5 = T_4\left(1 - \eta_{GT}\left[1 - \left(\frac{P_4}{P_5}\right)^{\frac{1-Y_g}{Y_g}}\right]\right) \tag{25}$$

$$W_{GT} = m_g\ C_{p,g}(T_4 - T_5) \tag{26}$$

$$W_{net} = W_{GT} - W_{AC} \tag{27}$$

Figure 3-4 represents the detailed schematic diagram of the HRSG and its connection with the steam turbine and the MED. The energy and mass balances for the economizer, evaporator, and superheater are given in (28), (29), and (30), respectively. To elaborate, (30) states that the energy transferred from hot gases to the cold water in the evaporator is equal to the energy transferred from the steam to the superheater. Precisely, the model involves the constraints demonstrated in (31), (32), and (33) to develop the temperature profiles within the HRSG.

$$m_g\ C_{pg}\ (T_{14} - T_7\ ) = m_s\ (h_9 - h_8) \tag{28}$$

$$m_g C_{p,g}(T_{13} - T_{14}) = m_s(h_{10} - h_9) \tag{29}$$

$$m_g C_{p,g}(T_6 - T_{13}) = m_s(h_{11} - h_{10}) \tag{30}$$

$$T_9 > T_8 \tag{31}$$

$$T_{10} = T_9 \tag{32}$$

$$T_{11} > T_{10} \tag{33}$$

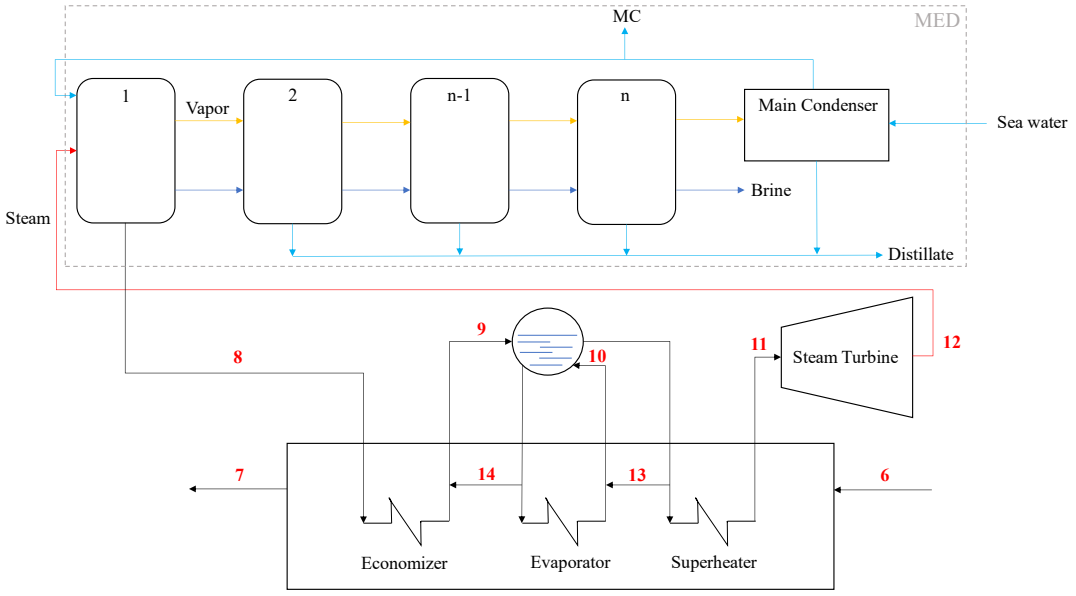

Figure 3-4: Schematic diagram of HRSG integrated with steam turbine and MED.

The modeling of the steam turbine mainly includes the thermodynamic properties of streams 11 and 12. Accordingly, (34) indicates the power of the steam turbine [52]. Essentially, constraint, shown in (35), ensures that the pressure of the steam entering the steam turbine is greater than that of the one exiting it.

$$W_{ST} = m_s\,(h_{11} - h_{12}\,)\eta_{st} \tag{34}$$

$$P_{11} > P_{12} \tag{35}$$

3.2.3. Mathematical Model of MED Plant

In the forward feed MED, the produced vapor from the first effect acts as a heat source, and the concentrated brine serves fully as the feed for the second effect. Furthermore, this feed gets concentrated, producing a vapor that performs as a heat source for the third effect, and this process continues till the brine is discharged at the last effect. In addition, from the last effect, the produced vapor is cooled in the main condenser, resulting in a distillate [16], [53], [54].

As shown in Figure 3-4, the steam coming out from the steam turbine acts as a heat source for the first effect of the MED. Equations (36) and (37) ensure the distillation effects' overall material and salt balances.

$$m_{feed}^{MED} = m_{dis} + B_{(6)} \tag{36}$$

$$X_f m_{feed} = B_{(6)} X_{last} \tag{37}$$

Equations (38), (39), and (40) establish the mass and energy balances in the distillation effects.

$$m_{feed}^{MED} = V_{(1)} + B_{(1)} \tag{38}$$

$$V_S L_s = V_1 L_{v(1)} \tag{39}$$

$$V_{(n)} L_{v(n)} = V_n L_{v(1)} \tag{40}$$

Accordingly, (41) and (42) calculate the heat transfer area in the first effect and other effects, where the latent heat of motive steam, L_s, and vapor, $L_{v(n)}$, is calculated using the correlation given in [16].

$$V_{(1)} L_{v(1)} = A_{(1)} \cdot U(T_s - T_{MED(1)}) \tag{41}$$

$$V_{(n)} L_{v(n)} = A_{(n)} \cdot U(T_{MED(n-l)} - T_{MED(n)}) \tag{42}$$

As previously mentioned, (43) and (44) imply that the brine acts as a feed for the next effect and calculate the brine flow rate leaving the previous effect.

$$B_{(n-1)} = V_{(n)} + B_{(n)} \tag{43}$$

$$B_{(n-1)} X_{(n-1)} = B_{(n)} X_{(n)} \tag{44}$$

Energy balances of the main condenser are defined in (45), (46), and (47), including the log mean temperature difference reported in [16].

$$A_{cond} \cdot U_{cond} \cdot T_{cond} = V_{(6)}\, L_{V(6)} \tag{45}$$

$$m_{sea} \cdot C_p (T_{cfeed} - T_{feed}) = V_{(6)} L_{V(6)} \tag{46}$$

$$m_{sea} = m_c + m_{feed}^{MED} \tag{47}$$

Most importantly, MED's model includes a constraint, (48), that ensures the temperature profile in effect $(n-1)$ is below the one in effect (n). Lastly, (49) expresses the total MED heat transfer area.

$$T_{MED(n-1)} > T_{MED(n)} \tag{48}$$

$$HTA_{MED} = A_{cond} + \sum_1^n A_{(n)} \tag{49}$$

3.3. Mathematical Model of Reverse Osmosis Desalination Plant

In this study, the RO is a single-stage desalination system and is made of six parallel vessels, each comprising six membranes. Mainly, the RO system consists of a high-pressure pumping unit that consumes significant electricity. A simple mathematical model that describes the process of RO desalination is derived from [16] and [55]. Accordingly, (50) and (51) establish the mass and salt balance of the permeate.

$$m_{feed}^{RO} = m_p + m_b \tag{50}$$

$$X_f m_{feed}^{RO} = X_p m_p + X_b m_b \tag{51}$$

Equation (52) calculates the rate of the water flow through one membrane, m_p, where the water permeability coefficient, K_w, is $2.05 \times 10^{-6}\, m^3/m^2\, s\, kPa$.

$$m_p = (\triangle P_h - \triangle \pi)\, K_w\, A_{RO} \tag{52}$$

The net hydraulic and osmotic pressures across the membrane are determined by (53) and (54), respectively.

$$\triangle P_h = 0.5\left(P_{h,f} + P_{h,b}\right) - P_{h,p} \tag{53}$$

$$\triangle \pi = 0.5\left(\pi_f + \pi_b\right) - \pi_p \tag{54}$$

Regarding salt transport, (55) defines the salt flow rate through the membrane, m_{salt}, where the average salinity on the feed side is calculated using (56). Moreover, (57) implies that the permeate's salinity, X_p, depends on the water and salt transport rates through the membrane.

$$m_{salt} = \left(X_{avg} - X_p\right) K_s\, A_{RO} \tag{55}$$

$$X_{avg} = \frac{(X_f m_{feed}^{RO} + X_b m_b)}{(m_{feed}^{RO} + m_b)} \tag{56}$$

$$X_p = \frac{m_{salt}}{m_p} \tag{57}$$

The salt rejection, SR, depicted in (58) is utilized to calculate the salinity of the permeate. Most importantly, the total water production, m_p^{total}, from the RO system is determined using (59), where n_{RO} is the total number of membranes in the system.

$$SR = 1 - \frac{X_p}{X_f} \tag{58}$$

$$m_p^{total} = n_{RO}\, m_p \tag{59}$$

Equation (60) estimates the specific power consumption of the high-pressure pumping unit where the seawater's density, ρ, is $1060\,\frac{kg}{m^3}$.

$$W_{RO} = \frac{n_{RO}\, P_{h,f}\, m_{feed}^{RO}}{\eta_{RO}\, \rho^s} \tag{60}$$

3.4. Mathematical Model of Reservoir

In this study, the distillate in kg/s produced from the MED system is considered uniform at all times, i.e., lumped approach, in order to develop a simplified and fast model. Equation (50) guarantees that the water demand at the current hour is fulfilled by the distillate added to the difference between the reservoir capacity at the previous and current hours. As illustrated in (61), factor 3.6 is added to convert the distillate flow rate from kg/s to m^3/h. Similarly, (62) carries out the exact correlation but with the initial capacity of the reservoir at the first hour; most importantly, to demonstrate a complete cycle, the capacity of the reservoir at the end of the current day should be nearly equal to its capacity at the beginning of the next day, i.e., $W_{res(24)} = W_{res(1)}$.

$$3.6\, m_{dis} + W_{res(t-1)} = W_{res(t)} + W_{demand(t)} \tag{61}$$

$$3.6\, m_{dis} + W_{res(24)} = W_{res(1)} + W_{demand(1)} \tag{62}$$

3.5. Integration of Power and Water Systems

After modeling electrical power and water systems, this subsection integrates both systems for co-optimizing both networks in a given micro-WEN. The power and water network integration is implemented in two stages. In the first stage, the CCPP and the MED system are integrated, whereas the second stage includes the integration of the CCPP, the MED, and the power generation network.

As elaborated in previous sections, the steam coming out from the steam turbine acts as a heat source for the first effect of the MED. Thus, this relation is added as a constraint in the integrated micro-WEN's model as expressed in (63), (64), (65), and (66).

$$m_s = V_s \tag{63}$$

$$T_{12} = T_s \tag{64}$$

$$T_{12} = T_8 \tag{65}$$

$$60 \leq T_s \leq 110 \tag{66}$$

Then, for integrating the CCPP and the IEEE-24 bus system, the total generated power from the gas and the steam turbines is injected into the buses where the cogeneration units are installed. Since the CCPP's model has the scale of a day, whereas the electrical network is time-based, the output power of the CCPP is the daily average generated power at bus i, as illustrated in (67).

$$\sum_{t=1}^{24} P_{i,t}^{g} = W_{net} + W_{ST} \tag{67}$$

3.6. Economic Models

This subsection presents the economic models used to evaluate the cost of the micro-WEN system. It is vital to consider the annual cost of the fuel used in the CCPP, the capital investment, and the maintenance costs to minimize the total annual cost of the plant. The economic model of the CCPP is obtained from previous studies [47], [56], [57]. Additionally, details of modeling the MED's economic performance are attained from recent literature [16], [50].

3.6.1. Economic Model of CCPP

Firstly, the purchase cost for the AC, the CC, the APH, the gas turbine, the HRSG, and the steam turbine are calculated respectively as follows:

$$Z_{AC} = \left(\frac{C_{11} m_a}{C_{12} - \eta_{AC}}\right)\left(\frac{P_2}{P_1}\right)\ln\left(\frac{P_2}{P1}\right) \tag{68}$$

$$Z_{CC} = \left(\frac{C_{21} m_a}{C_{22} - \frac{P_4}{P_5}}\right)(1 + EXP[C_{23} T_4 - C_{24}]) \tag{69}$$

$$Z_{APH} = C_{41}\left(\frac{m_g (h_5 - h_6)}{U \triangle TLM_{APH}}\right)^{0.6} \tag{70}$$

$$Z_{GT} = \left(\frac{C_{31} m_g}{C_{32} - \eta_{GT}}\right)\ln\left(\frac{P_4}{P_5}\right)(1 + EXP[C_{33} T_4 - C_{34}]) \tag{71}$$

$$Z_{HRSG} = C_{51}\left[\left(\frac{m_g C_{p,g}(T_{14}-T_7)}{\triangle TLM_{ECO}}\right)^{0.8} + \left(\frac{m_g C_{p,g}(T_6-T_{13})}{\triangle TLM_{EV}}\right)^{0.8} + \left(\frac{m_g C_{p,g}(T_{13}-T_{14})}{\triangle TLM_{SH}}\right)^{0.8}\right] + C_{52}m_s + C_{53}m_g^{1.2} \quad (72)$$

$$Z_{ST} = C_{61}W_{ST}^{0.7}\left(1+\left(\frac{0.05}{1-\eta_{ST}}\right)^3\right)\left(1+5\cdot EXP\left[\frac{T_{11}-866}{10.42}\right]\right) \quad (73)$$

As shown above, the purchase cost of each component is calculated by multiplying the appropriate variables, such as mass flow rates, pressure ratios, and temperatures, by specific cost constants, C, which are typically based on historical data or estimates of the costs associated with each component.

Then, the total annual cost of the CCPP is estimated by (74) where c_f is the fuel cost per energy unit with a value of $0.004\ \$/MJ$.

$$TAC_{CCPP} = 3600\ N_{CCPP}\ c_f m_f LHV + CRF\ MTF\ (Z_{AC} + Z_{CC} + Z_{GT} + Z_{HRSG} + Z_{APH} + Z_{ST}) \quad (74)$$

3.6.2. Economic Model of MED

To compute the total annual investment cost of the MED system, both the indirect and direct capital costs are taken into consideration. As illustrated and simplified in (75), the direct capital cost includes the total equipment cost and the civil work capital cost. In contrast, the indirect capital cost is estimated to be one-fourth of the direct one.

$$TCC_{MED} = 1.25\ (CC_{eq} + CC_{cw}) \quad (75)$$

As mentioned previously, the desalination system consists of a MED unit and a main condenser. Also, CC_{eq} considers the cost related to the equipment that absorbs and pre-treats the seawater. So, CC_{eq} and CC_{cw} are expanded to:

$$CC_{eq} = CC_{swip} + CC_{MED} + CC_{cond} \quad (76)$$

$$CC_{cw} = 0.15\ CC_{eq} \quad (77)$$

Consequently, (78), (79), and (80) calculate the cost of each equipment that is prementioned.

$$CC_{swip} = \frac{24\ 3600\ Cswip\ m_{feed}}{\rho^{b}} \tag{78}$$

$$CC_{MED} = C_{mat,MED}\ K_{MED} \left(\sum_{1}^{n} A_{(n)} \right)^{scal_{MED}} \tag{79}$$

$$CC_{cond} = C_{mat,Cond}\ K_{Cond}\ A_{cond}{}^{scal_{Cond}} \tag{80}$$

Moreover, the annual operating cost of the MED is estimated by:

$$AOC_{\mathrm{MED}} = OC_{epow} + OC_{st} + OC_{lab} + OC_{man} + OC_{ins} \tag{81}$$

The annual cost of electric power, steam, labor, maintenance, and insurance is represented in (82), (83), (84), (85), and (86) correspondingly.

$$OC_{epow} = 365\ C_{e}\ W_{MED}\ f\ m_{Dis} \tag{82}$$

$$OC_{st} = 3600\ C_{st}\ N_{MED}\ \frac{T_{s} - 40}{80}\ V_{s} \tag{83}$$

$$OC_{lab} = 3600\ C_{lab}\ \frac{N_{MED}}{\rho^{p}}\ m_{Dis} \tag{84}$$

$$OC_{man} = 0.001\ TCC_{MED} \tag{85}$$

$$OC_{ins} = 0.005\ TCC_{MED} \tag{86}$$

Lastly, the total annual cost of the MED system is evaluated as:

$$TAC_{MED} = CRF\ TCC_{MED} + AOC_{MED} \tag{87}$$

Chapter 4. Cases Studies and Simulation Results

In this chapter, two possible approaches are introduced to optimize the proposed micro-WEN system's design and operation based on the mathematical models proposed previously in Chapter 3. Firstly, for an optimal design, the total annual cost of the developed micro-WEN system is minimized by optimizing the design of the CCPP and MED system while meeting the daily electrical and water demand. Secondly, the proposed micro-WEN system is co-optimized for optimal operation of the system to acquire the minimum total operational cost with and without a PV system. The optimization models and the solving approaches are implemented in the GAMS modeling environment and solved using the CONOPT solver.

4.1. Optimal Design of a Micro-WEN System

The proposed micro-WEN system is co-optimized as an integrated physical system with the aim of minimizing its total annual cost and meeting the daily electricity and water demand.

Firstly, before optimizing, model variables of the following model are initialized to values reported in recent and related works to acquire feasible initial solutions that satisfy mass and energy balances in each component of the MED system and the CCPP. Accordingly, in developing a simulation model, no objective function is considered. Then, the feasible solution obtained for the model is used as an initialization point to minimize the total annual cost of the micro-WEN system. Thus, the optimization model can be defined as in (88).

$$\left.\begin{array}{c} min\ TAC_{WEN} = TAC_{CCPP} + TAC_{MED} \\ Subject\ to\ (1) - (49)\ \ and\ \ (61) - (87) \end{array}\right\} \quad (88)$$

Applying the co-optimization approach, Table 4-1 summarizes the optimum design values of the MED system and the CCPP that meet a typical daily electrical and water load. The optimal distribution among the capital investment and operating costs that results in the minimal total annual cost of the micro-WEN system is outlined in Table 4-2.

Table 4-1: Optimum values of design variables of micro-WEN system.

Design variables		Value
MED	n_{MED}	6
	HTA_{MED}	5,985 m^2
CCPP	η_{GT}	54.9%
	η_{ST}	96.5%
	W	150 MW
RO	n_{RO}	36
	A_{RO}	197.88 m^2

Table 4-2: Capital investment and operating costs of micro-WEN system.

System	Capital Investment ($/year)	Operating cost ($/year)
MED	1.82 M	1.12 M
CCPP	0.86 M	3.5 M
Micro-WEN	5.91 M	

Fulfilling the demand from both the energy and water sectors, the designed cogeneration unit's water and electricity production capacity is 145 m^3/h and 150 MW, respectively. The capacity of the electrical network, the IEEE 24-bus system, is 2890 MW, whereas its maximum demand is 2850 MW. Figure 4-1 represents the generated power at each bus.

Different case studies are investigated to estimate the number of cogeneration units that are required to replace the generating units of the IEEE-24 bus system while considering several percentages of the electricity consumed by the residential sector. According to [58], residents typically use about 0.55 m^3 of water and 25 kWh of electricity daily. In the UAE, the consumption of the residential sector in an emirate accounted for 26.8% of the total consumption [59]. Considering 26.8%, 50%, and 100% for the residential electricity consumption, Table 4-3 summarizes the number of

households that the electrical system can serve, their daily water consumption, and the number of cogeneration units that satisfy these households' water consumption.

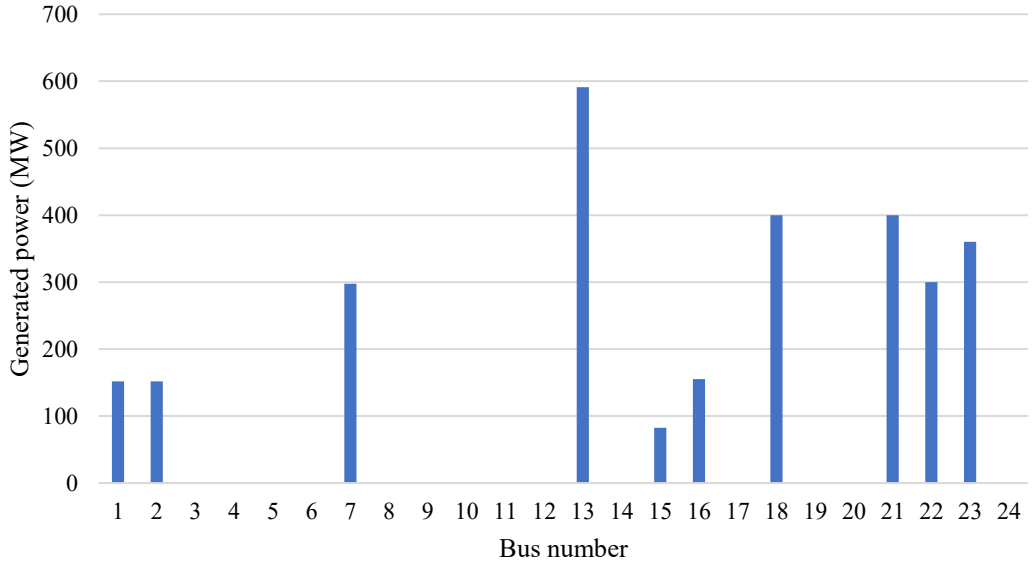

Figure 4-1: Generated power at each bus with no cogeneration units.

Table 4-3: Various percentages of electricity consumption by the residential sector.

	No. of households	**Daily water consumption (m^3/day)**	**No. of cogeneration units**
26.8%	30,984	17,041.2	5
50%	57,806	31,793.3	17
100%	115,612	63,538.6	19

As illustrated in Table 4-3, five cogeneration units with a total capacity of 750 MW are required to satisfy the water demand of 30,984 households. Thus, as shown in Figure 4-3, the generating units at buses 15, 22, and 23, with a corresponding capacity of 82 MW, 300 MW, and 360 MW, are replaced with five cogeneration units at buses 5, 15, 19, 22, and 23.

Increasing the number of households increases the required number of cogeneration units proportionally intending to meet the daily water load. Hence, 57,806 households require 31,793.3 m3/day, which seventeen cogeneration units supply. Therefore, as

presented in Figure 4-2, seventeen cogeneration units are added and replaced all generating units of the IEEE 24-bus system except the generator at bus 23.

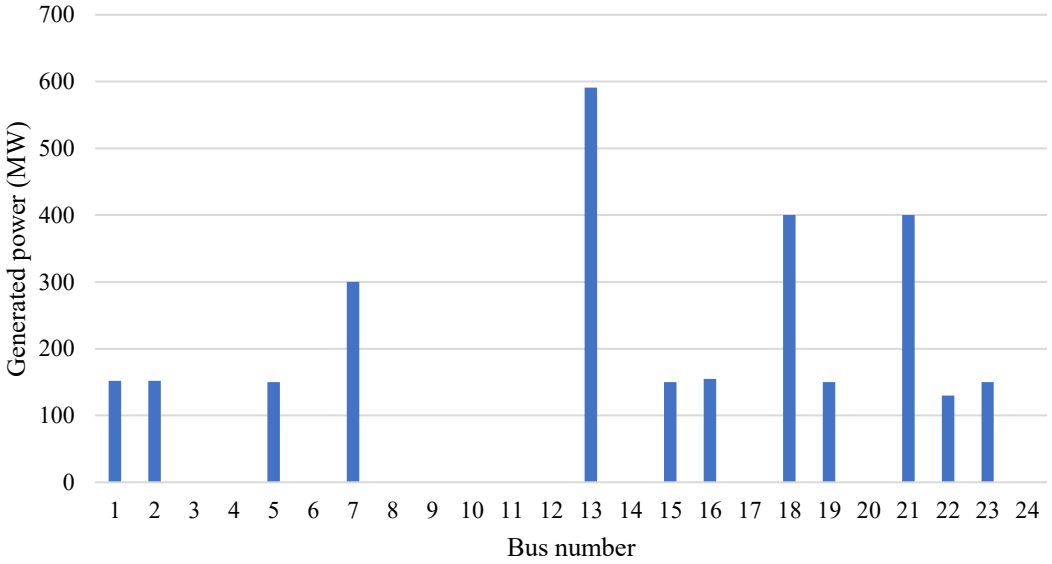

Figure 4-2: Generated power at each bus with five cogeneration units.

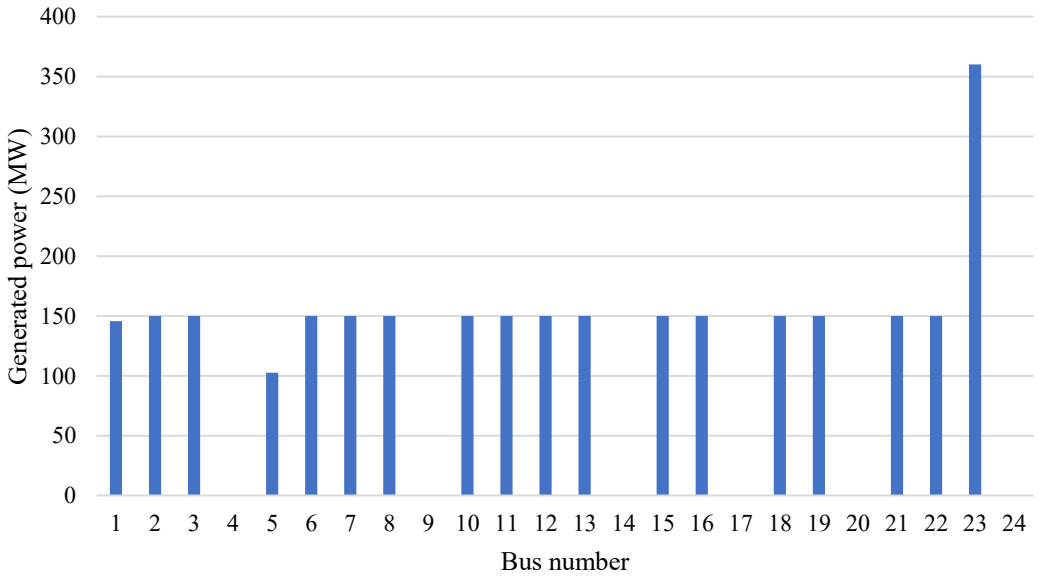

Figure 4-3: Generated power at each bus with seventeen cogeneration units.

Lastly, to meet the electrical and water demands of an area that considers only the residential sector, nineteen cogeneration units replace all the generating units of the electrical network. They are located on the buses that are depicted in Figure 4-4.

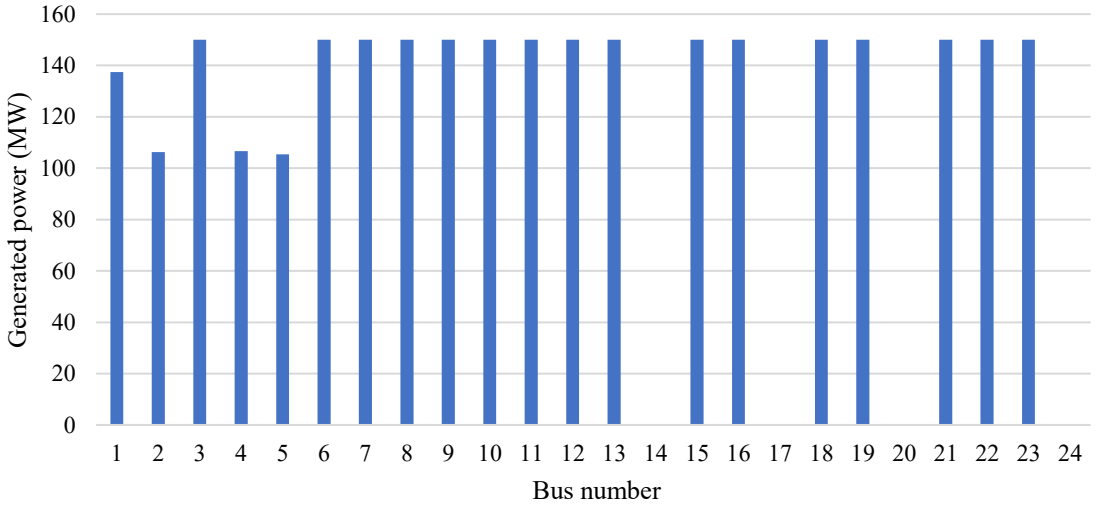

Figure 4-4: Generated power at each bus with a cogeneration unit.

4.2. Integration of PV

The generation network is integrated with a renewable energy resource to investigate its effect on meeting the electrical and water demands the cogeneration unit should satisfy. A PV system's typical average output curve is shown in Figure 4-5, where the power generated from the PV system depends on solar irradiance [60]. Hence, as illustrated in Figure 4-6, a PV system with a capacity of 50 MW is added to the proposed micro-WEN system at bus 17. To include the PV system, the electrical network's active and reactive power balance constraints are modified, as demonstrated in (89) and (90).

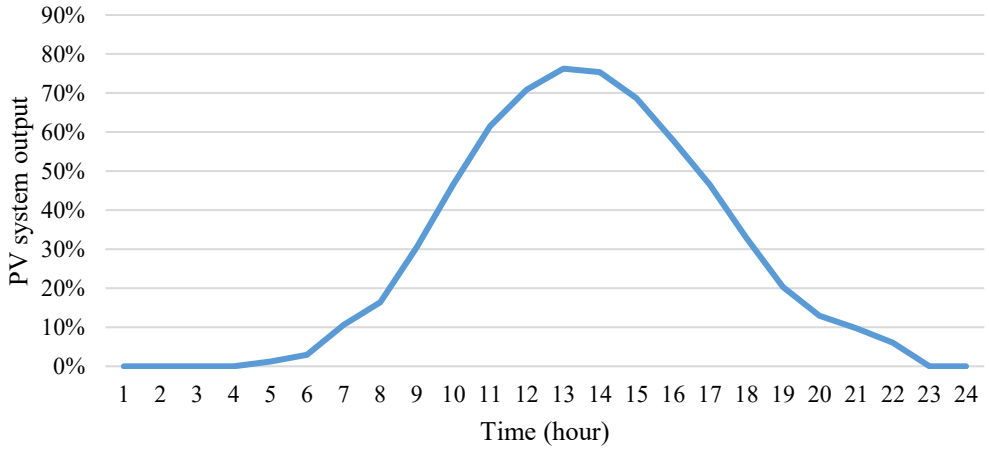

Figure 4-5: Curve of PV Output power.

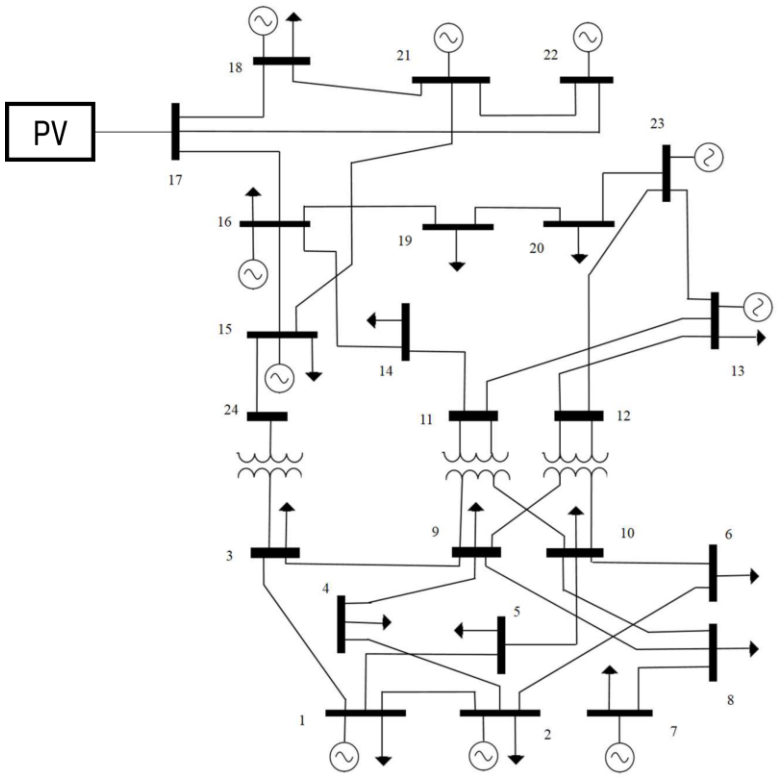

Figure 4-6: Integration of PV System and IEEE 24-bus system.

$$P_{i,t}^{PV} + P_{i,t}^{g} - P_{i,t}^{L} = \sum_{j \epsilon \Omega^{i}} P_{ij,t} \tag{89}$$

$$Q_{i,t}^{PV} + Q_{i,t}^{g} - Q_{i,t}^{L} = \sum_{j \epsilon \Omega^{i}} Q_{ij,t} \tag{90}$$

To compare the difference in the generated power at each bus before and after integrating the PV system with the proposed micro-WEN system that serves households of 26.8%, Figure 4-7 and Figure 4-8 represent the hourly generated power at each bus and the hourly output power of the PV system respectively.

As presumed, after adding the PV system, it can be inferred that the generated power at the buses where the cogeneration units are located decreases between 9 AM to 5 PM, during which the PV system supplies power to the electrical network. For instance, Figure 4-9 clearly shows the difference in the cogeneration unit's generated power located at bus 23 without and with the integration of a PV system, especially from 10 AM to 5 PM. However, suppose a PV system of a significant size generates the amount of electricity that is provided by a cogeneration unit and results in turning it off. In that case, the freshwater the cogeneration units produce won't satisfy the water demand. Therefore, to address this problem, it is proposed to decouple the electricity and water

production by phasing out the cogeneration units and shifting to the reverse osmosis desalination technique.

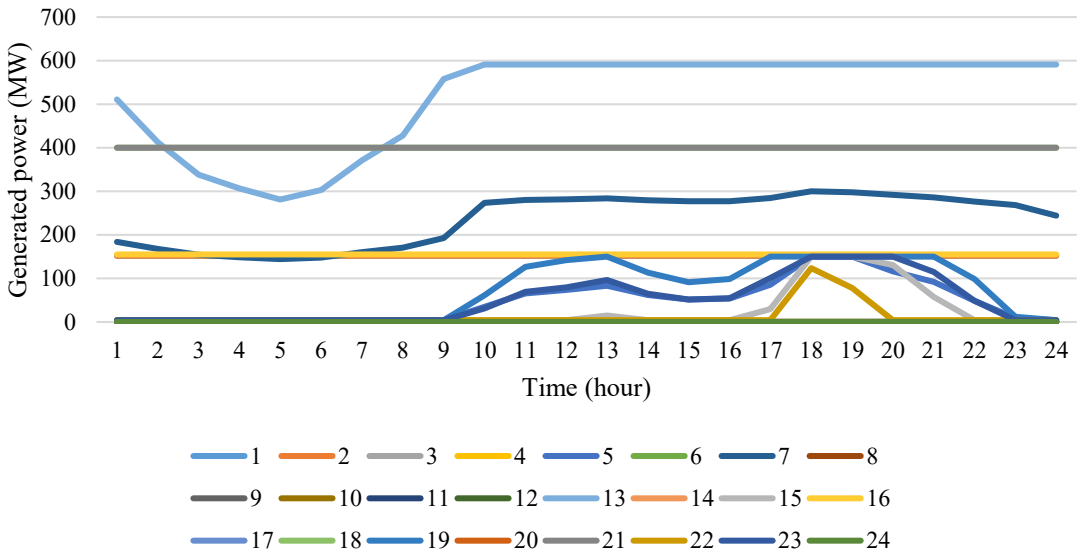

Figure 4-7: Hourly generated power at each bus with PV system.

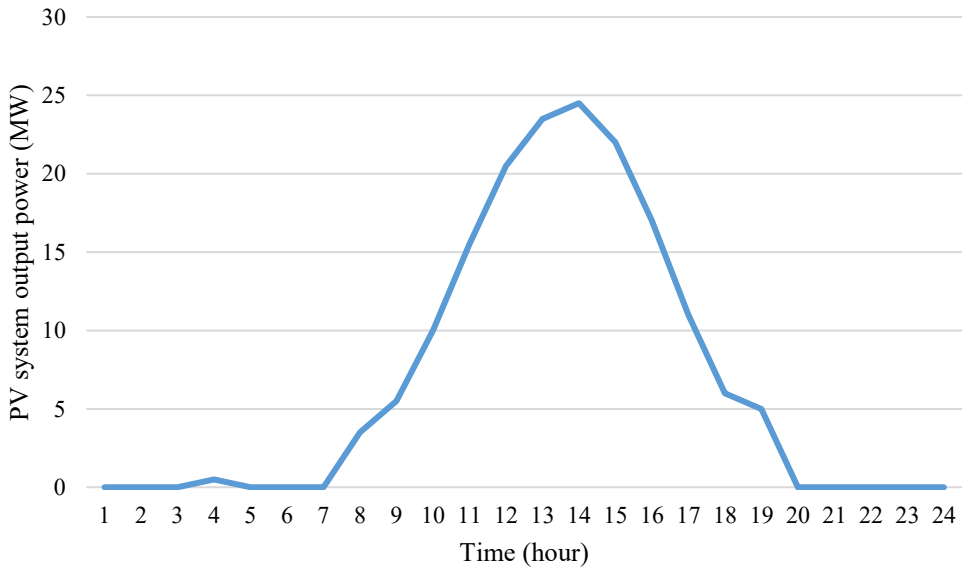

Figure 4-8: Hourly output power of PV system.

4.3. Shifting to Reverse Osmosis

As discussed earlier, thermal desalination plants satisfy the water demand of most of the residential sector in the UAE, and these desalination systems are typically part of combined-cycle cogeneration thermal plants. However, suppose any other source provides the amount of electricity that the cogeneration unit generates, and they are

consequently turned off. In that case, the freshwater the cogeneration units produce won't satisfy the water demand. Similarly, in Figure 4-10, the electric demand is severely reduced during winter, but the water demand doesn't change compared to other seasons. Consequently, UAE operates its power plants during the winter at low efficiency to be able to meet the water demand. Thus, this work proposes to shift to more sustainable water desalination and decouple electricity and water production. The best approach is shifting from thermal desalination to RO, which consumes significant electricity. Nevertheless, any renewable energy resource such as a PV system or a storage system like a battery may provide this electricity to produce water. Thus, water desalination won't rely on thermal energy from a CCPP.

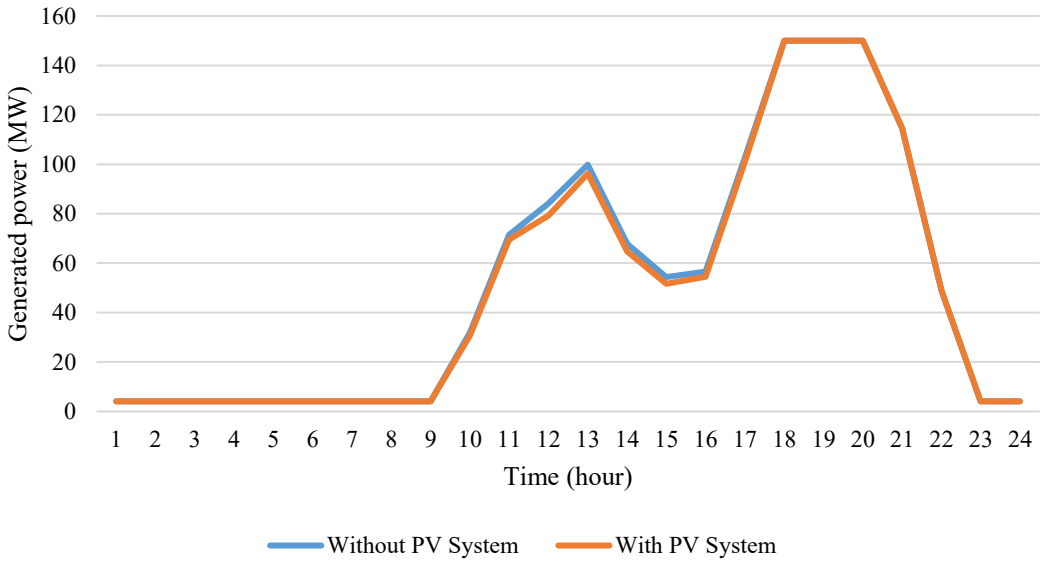

Figure 4-9: Generated power at bus 23 without and with PV system.

The electrical network's real and reactive power balance constraints are further modified as described by (91) and (92) to add the active and reactive power consumptions of the water pump, which is connected to the IEEE-24 bus system at bus 7.

$$P_{i,t}^{PV} + P_{i,t}^{g} - P_{i,t}^{L} - P_{7,t}^{RO} = \sum_{j \epsilon \Omega^{i}} P_{ij,t} \tag{91}$$

$$Q_{i,t}^{PV} + Q_{i,t}^{g} - Q_{i,t}^{L} - Q_{7,t}^{RO} = \sum_{j \epsilon \Omega^{i}} Q_{ij,t} \tag{92}$$

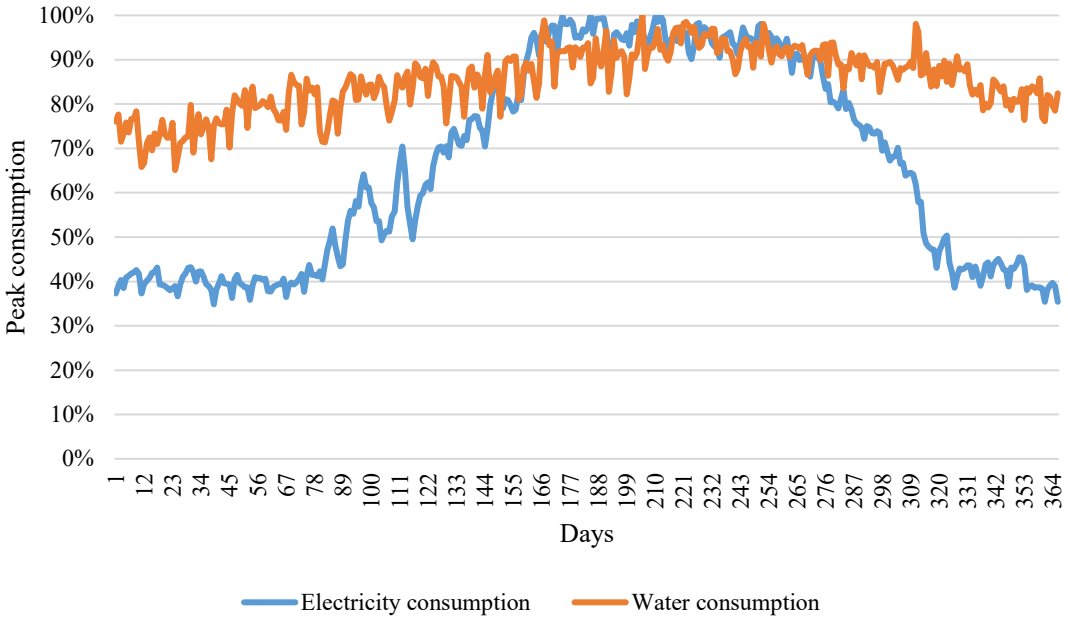

Figure 4-10: Electricity vs. water consumption.

The reservoir has an initial capacity of 190.25 m^3 and is supplied hourly with a constant permeate of 145.48 m^3. Consequently, as shown in Figure 4-11, the RO system satisfies the water demand regardless of integrating a PV system compared to cogeneration units.

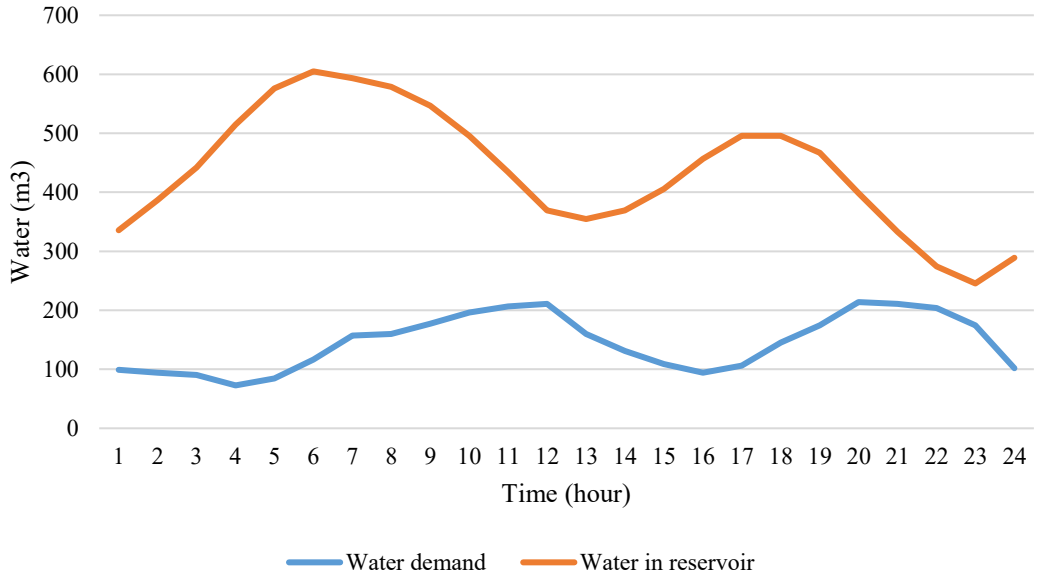

Figure 4-11: Water demand vs. water in reservoir.

This work considers seasonal variations as the electricity demand varies depending on the season. It displays the year as four days, a total of 96-hour slots, where each day

represents a season, and each day constitutes 24-hour slots. The normalized electrical demand of each season sample day is displayed in Figure 4-12. To meet the water demand, the water pump consumes electricity of 887.144 kWh and to pump a feed of 362.75 m^3/h. On that account, considering a unity power factor of 0.98, the reactive power is compensated in water pumps and RO system.

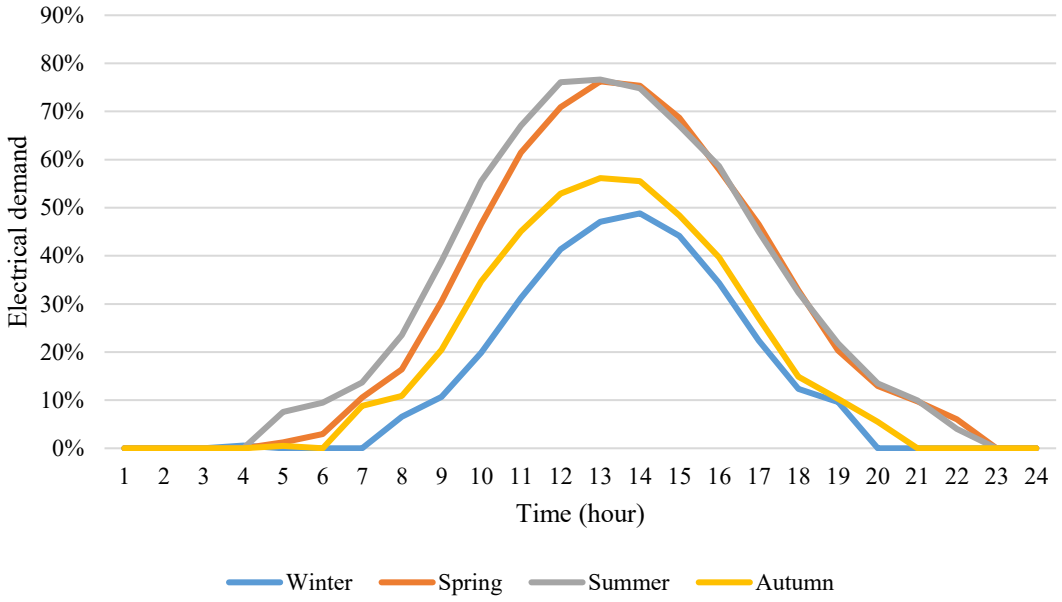

Figure 4-12: Seasonal electric demand.

It can be inferred from Figure 4-13 that the generated power at bus 7 increases after connecting the water pump to the electrical network to supply active power. Then, adding a PV system reduces the power generated at the bus as it provides additional active power to the electrical network.

4.4. Optimal Operation of a Micro-WEN System

Furthermore, the proposed micro-WEN system is co-optimized to minimize its total operational cost, defined in (93), where the 24-hour electricity price at the power transmission bus, p_e, is shown in Figure 4-14.

$$\left.\begin{aligned} min\ OC_{WEN} = \sum_{i,t} b_g\, P_{i,t}^{g}\, S_{base} + \sum_{t} p_e W_{RO} \\ Subject\ to\ (1)-(12), (50)-(62), \text{and } (89)-(92) \end{aligned}\right\} \quad (93)$$

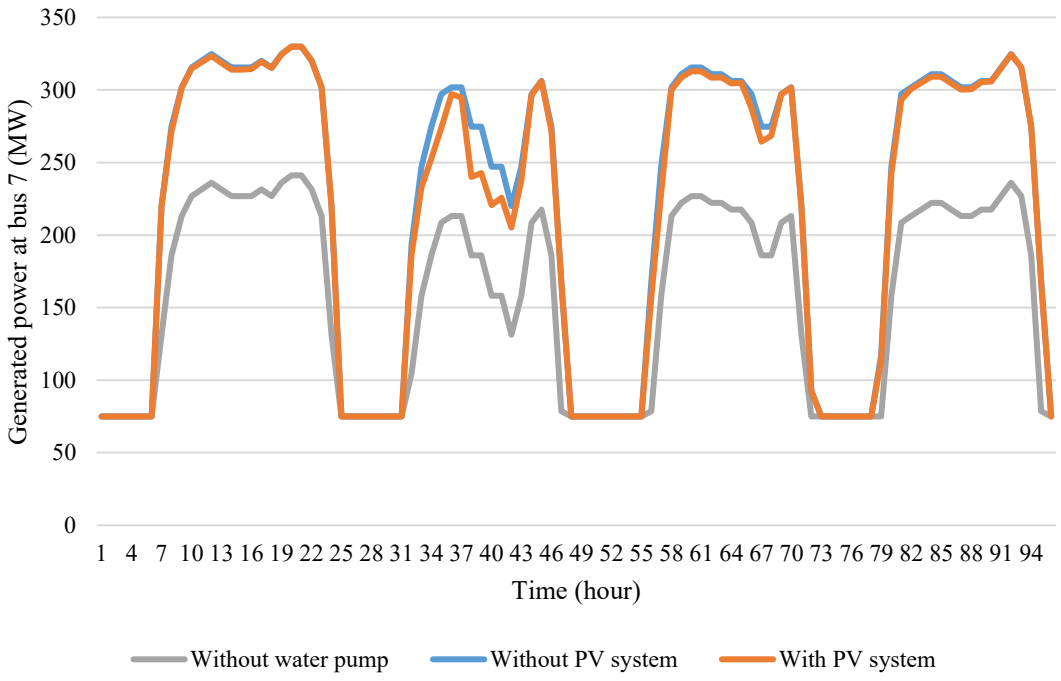

Figure 4-13: Hourly generated power at bus 7.

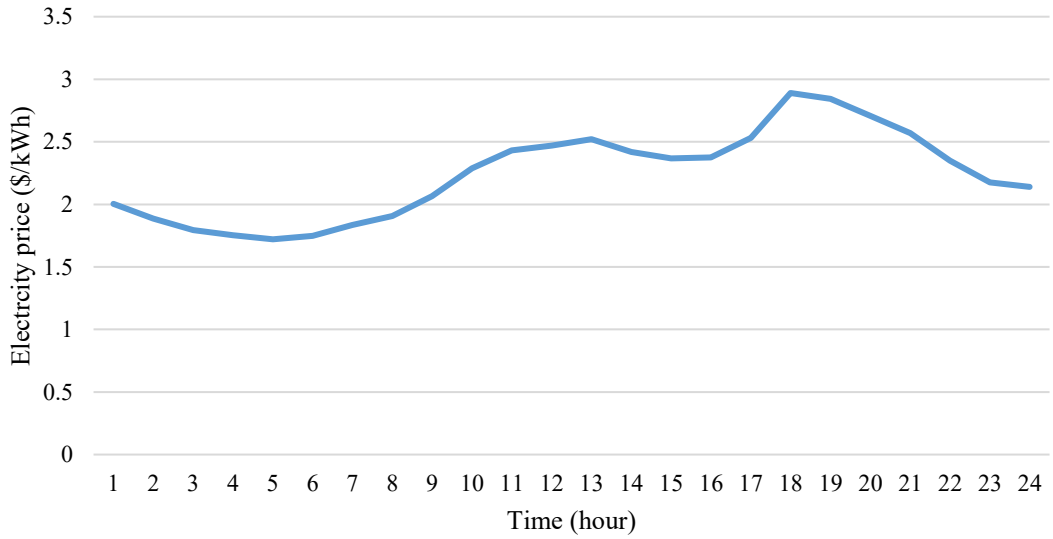

Figure 4-14: Hourly electricity price.

Before optimizing, as reported in Table 4-4, model variables of the CCPP and MED system are bounded within lower and upper bounds from recent and related literature. With the proposed co-optimization model implemented, the optimal operating conditions of all flows, such as mass flow rates, temperature, and pressure, are summarized in Table 4-3.

Table 4-4: Lower and upper bounds of operating conditions of micro-WEN system.

Operating Conditions		Lower Bounds	Upper Bounds
MED	T_{cfeed}	30 °C	80 °C
	$T_{MED(n)}$	36 °C	130 °C
	$L_{v(n)}$	2,000 kJ/kg	3,000 kJ/kg
	T_s	80 °C	150 °C
CCPP	W_{net}	30 MW	-
	W_{ST}	11 MW	-
	T_k	298.15 K	1500 K
	m_a	94 kg/s	-

Table 4-5 highlights the minimum operating cost of the proposed micro-WEN system without and with a PV system. Also, the total operating cost of the micro-WEN when the RO system replaces the cogeneration units to satisfy the water demand is defined. As a result, according to Table 4-6, co-optimizing the overall system with PV saves approximately 0.01 M, and phasing out the cogeneration units and shifting to the RO system leads to a reduction of 26.7% in the total operational cost of the proposed micro-WEN system.

Table 4-5: Optimum values of operating conditions of micro-WEN system.

Operating Conditions		Value
MED	m_{feed}^{MED}	136.65 kg/s
	V_s	63.193 kg/s
	m_{dis}	40.41 kg/s
	T_s	110 °C
CCPP	m_s	6.42 kg/s
	m_f	0.601 kg/s
	m_a	41.86 kg/s
	T_{12}	383.15 K
	P_{11}	1.101 bar

	P_{12}	0.101 bar
RO	m_{feed}^{RO}	2.8 kg/s
	m_b	1.68 kg/s
	m_p	1.12 kg/s
	SR	99.6%

Table 4-6: Comparison of total operating cost of micro-WEN system.

	Total operating cost ($/day)
Without PV	0.82 M
With PV	0.81 M
Shifting to RO	0.61 M

Chapter 5. Conclusion and Future Work

To conclude, by 2050, there is expected to be an increase of 2 billion in the world's population. Consequently, this would result in a rise in energy and water demand, and it is approximated that water scarcity is expected to affect roughly 40% of the world's population. The optimal operation of a micro water-energy nexus (WEN) system is crucial in addressing the increasing demand for water and energy. Accordingly, the integration of thermal desalination of seawater in the combined cycle power generation plant is a promising solution for both power generation and water desalination. Most importantly, novel and robust resource management must be employed to reduce the micro-WEN system's total annual cost as well as to optimize the use of energy resources. As a result, this thesis proposes an NLP mathematical model for the generation-level micro-WEN system with a co-optimization framework for its design and operation to meet loads of the electrical and water networks at a minimum cost. Also, the issue of operating the UAE's power plants throughout the winter at low efficiency in order to be able to satisfy the water demand is addressed in this study by shifting from thermal desalination to RO desalination and decoupling the production of energy and water. According to the simulation results, the co-optimization model considerably reduces the overall operational cost by 1.23% and 26.7% with the integration of PVs and the switch to RO, respectively. Most importantly, optimizing the micro-WEN system over multiple timescales, such as hourly and daily, provides solutions with a significantly smaller memory size and requires less computational time.

In future work, other renewable resources like CSP shall be considered in the micro-WEN's model to supply thermal energy to thermal desalination, shifting for a low carbon footprint WEN. Moreover, future research shall include different energy storage technologies and electric vehicles within the WEN system for future smart communities.

References

[1] United States Department of Energy, "The Water-Energy Nexus: Challenges and Opportunities Overview and Summary," 2014, [Online]. Available: http://energy.gov/sites/prod/files/2014/07/f17/Water Energy Nexus Executive Summary July 2014.pdf, Accessed: November 5, 2022.

[2] G. Olsson, *Water and Energy*. IWA Publishing, pp. 1–13, 2015.

[3] A. Siddiqi and L. D. Anadon, "The water-energy nexus in Middle East and North Africa," *Energy Policy*, vol. 39, no. 8, pp. 4529–4540, 2011, doi: 10.1016/j.enpol.2011.04.023.

[4] J. M. Peterson, "Water-Energy-Food Nexus-Commonalities and Differences in the United States and Europe," *Compet. Water Resour. Exp. Manag. Approaches US Eur.*, pp. 252–258, 2017, doi: 10.1016/B978-0-12-803237-4.00014-8.

[5] IRENA, "Renewable energy in the water, energy and food nexus," *Int. Renew. Energy Agency*, no. January, pp. 1–125, 2015.

[6] R. Gonzalez Sanchez, R. Seliger, F. Fahl, L. De Felice, T. B. M. J. Ouarda, and F. Farinosi, "Freshwater use of the energy sector in Africa," *Appl. Energy*, vol. 270, no. February, p. 115171, 2020, doi: 10.1016/j.apenergy.2020.115171.

[7] M. Z. Jacobson and M. A. Delucchi, "Providing all global energy with wind, water, and solar power, Part I: Technologies, energy resources, quantities and areas of infrastructure, and materials," *Energy Policy*, vol. 39, no. 3, pp. 1154–1169, 2011, doi: 10.1016/j.enpol.2010.11.040.

[8] E. J. Okampo and N. Nwulu, "Optimisation of renewable energy powered reverse osmosis desalination systems: A state-of-the-art review," *Renew. Sustain. Energy Rev.*, vol. 140, no. September 2019, p. 110712, 2021, doi: 10.1016/j.rser.2021.110712.

[9] Z. Wang, L. Wang, and M. Elimelech, "Viability of Harvesting Salinity Gradient (Blue) Energy by Nanopore-Based Osmotic Power Generation," *Engineering*, vol. 9, pp. 51–60, 2022, doi: 10.1016/j.eng.2021.02.016.

[10] S. Mohyudin, R. Farooq, F. Jubeen, T. Rasheed, M. Fatima, and F. Sher, "Microbial fuel cells a state-of-the-art technology for wastewater treatment and bioelectricity generation," *Environ. Res.*, vol. 204, no. PD, p. 112387, 2022, doi: 10.1016/j.envres.2021.112387.

[11] W. Qi, J. Liu, and P. D. Christofides, "A distributed control framework for smart grid development: Energy/water system optimal operation and electric grid integration," *J. Process Control*, vol. 21, no. 10, pp. 1504–1516, 2011, doi: 10.1016/j.jprocont.2011.05.010.

[12] M. M. El-Halwagi, *Water–Energy Nexus for Thermal Desalination Processes*. 2017.

[13] B. T. Aklilu and S. I. Gilani, "Mathematical modeling and simulation of a cogeneration plant," *Appl. Therm. Eng.*, vol. 30, no. 16, pp. 2545–2554, 2010,

doi: 10.1016/j.applthermaleng.2010.07.005.

[14] A. Santhosh, A. M. Farid, and K. Youcef-Toumi, "Real-time economic dispatch for the supply side of the energy-water nexus," *Appl. Energy*, vol. 122, pp. 42–52, 2014, doi: 10.1016/j.apenergy.2014.01.062.

[15] W. in the West, "Water and Energy Nexus: A Literature Review," 2013. [Online]. Available: https://waterinthewest.stanford.edu/sites/default/files/Water-Energy_Lit_Review.pdf, pp. 14–17, Accessed: October 10, 2022.

[16] H. T. El-Dessouky and H. M. Ettouney, *Fundamentals of Salt Water Desalination*. Elsevier, 2002.

[17] K. Elsaid, M. Kamil, E. T. Sayed, M. A. Abdelkareem, T. Wilberforce, and A. Olabi, "Environmental impact of desalination technologies: A review," *Sci. Total Environ.*, vol. 748, p. 141528, 2020, doi: 10.1016/j.scitotenv.2020.141528.

[18] M. Qasim, M. Badrelzaman, N. N. Darwish, N. A. Darwish, and N. Hilal, "Reverse osmosis desalination: A state-of-the-art review," *Desalination*, vol. 459, no. February, pp. 59–104, 2019, doi: 10.1016/j.desal.2019.02.008.

[19] S. F. Ahmed *et al.*, "Strategies to improve membrane performance in wastewater treatment," *Chemosphere*, vol. 306, no. June, p. 135527, 2022, doi: 10.1016/j.chemosphere.2022.135527.

[20] A. Inayat and M. Raza, "District cooling system via renewable energy sources: A review," *Renew. Sustain. Energy Rev.*, vol. 107, no. June 2018, pp. 360–373, 2019, doi: 10.1016/j.rser.2019.03.023.

[21] U. Çakir, K. Çomakli, and F. Yüksel, "The role of cogeneration systems in sustainability of energy," *Energy Convers. Manag.*, vol. 63, pp. 196–202, 2012, doi: 10.1016/j.enconman.2012.01.041.

[22] P. Breeze, *Gas-Turbine Power Generation*. Elsevier, 2016.

[23] H. B. Harandi, A. Asadi, M. Rahnama, Z. G. Shen, and P. C. Sui, "Modeling and multi-objective optimization of integrated MED–TVC desalination system and gas power plant for waste heat harvesting," *Comput. Chem. Eng.*, vol. 149, p. 107294, 2021, doi: 10.1016/j.compchemeng.2021.107294.

[24] M. Aliyu, G. Hassan, S. A. Said, M. U. Siddiqui, A. T. Alawami, and I. M. Elamin, "A review of solar-powered water pumping systems," *Renew. Sustain. Energy Rev.*, vol. 87, no. August 2017, pp. 61–76, 2018, doi: 10.1016/j.rser.2018.02.010.

[25] UN Water, "Annual Report 2014," 2014. [Online]. Available: https://www.unwater.org/sites/default/files/app/uploads/2017/05/ANNUAL_REPORT_2014_Final.pdf, pp. 6–9, Accessed: January 12, 2023.

[26] IRENA, "Water Desalination Using Renewable Energy," 2012. [Online]. Available: www.etsap.org-www.irena.org.

[27] P. Zhao *et al.*, "Water-Energy Nexus Management for Power Systems," *IEEE Trans. Power Syst.*, vol. 36, no. 3, pp. 2542–2554, 2021, doi:

10.1109/TPWRS.2020.3038076.

[28] H. Mehrjerdi, "Modeling and optimization of an island water-energy nexus powered by a hybrid solar-wind renewable system," *Energy*, vol. 197, p. 117217, 2020, doi: 10.1016/j.energy.2020.117217.

[29] Z. H. Alnahhal, M. F. Shaaban, M. Hamouda, and M. Mokhtar, "Optimal Operation of Power System Integrated with Reverse Osmosis Water Desalination," *Proc. 2021 6th Int. Symp. Environ. Energies Appl. EFEA 2021*, pp. 6–10, 2021, doi: 10.1109/EFEA49713.2021.9406237.

[30] C. Wang, N. Gao, J. Wang, N. Jia, T. Bi, and K. Martin, "Robust Operation of a Water-Energy Nexus: A Multi-Energy Perspective," *IEEE Trans. Sustain. Energy*, vol. 11, no. 4, pp. 2698–2712, 2020, doi: 10.1109/TSTE.2020.2971259.

[31] F. Moazeni and J. Khazaei, "Co-optimization of wastewater treatment plants interconnected with smart grids," *Appl. Energy*, vol. 298, no. February, p. 117150, 2021, doi: 10.1016/j.apenergy.2021.117150.

[32] F. Mohammadi, M. Sahraei-Ardakani, Y. M. Al-Abdullah, and G. T. Heydt, "Coordinated Scheduling of Power Generation and Water Desalination Units," *IEEE Trans. Power Syst.*, vol. 34, no. 5, pp. 3657–3666, 2019, doi: 10.1109/TPWRS.2019.2901807.

[33] A. S. Tayerani Charmchi, P. Ifaei, and C. K. Yoo, "Smart supply-side management of optimal hydro reservoirs using the water/energy nexus concept: A hydropower pinch analysis," *Appl. Energy*, vol. 281, no. August 2020, p. 116136, 2021, doi: 10.1016/j.apenergy.2020.116136.

[34] D. Fooladivanda and J. A. Taylor, "Energy-optimal pump scheduling and water flow," *IEEE Trans. Control Netw. Syst.*, vol. 5, no. 3, pp. 1016–1026, 2018, doi: 10.1109/TCNS.2017.2670501.

[35] C. Mkireb, A. Dembélé, A. Jouglet, and T. Denoeux, "Robust Optimization of Demand Response Power Bids for Drinking Water Systems," *Appl. Energy*, vol. 238, no. October 2018, pp. 1036–1047, 2019, doi: 10.1016/j.apenergy.2019.01.124.

[36] A. A. Atia and V. Fthenakis, "Active-salinity-control reverse osmosis desalination as a flexible load resource," *Desalination*, vol. 468, no. July, p. 114062, 2019, doi: 10.1016/j.desal.2019.07.002.

[37] R. Menke, E. Abraham, P. Parpas, and I. Stoianov, "Extending the Envelope of Demand Response Provision though Variable Speed Pumps," *Procedia Eng.*, vol. 186, pp. 584–591, 2017, doi: 10.1016/j.proeng.2017.03.274.

[38] C. Li, Y. Yao, K. Xie, B. Hu, and T. Niu, "Integrated Electrical, Heating, and Water Distribution System to Accommodate Wind Power," *IEEE Trans. Sustain. Energy*, vol. 12, no. 2, pp. 1100–1114, 2021, doi: 10.1109/TSTE.2020.3034134.

[39] D. Fooladivanda, A. D. Dominguez-Garcia, and P. W. Sauer, "Utilization of Water Supply Networks for Harvesting Renewable Energy," *IEEE Trans. Control Netw. Syst.*, vol. 6, no. 2, pp. 763–774, 2019, doi: 10.1109/TCNS.2018.2873946.

[40] K. Oikonomou and M. Parvania, "Optimal Participation of Water Desalination Plants in Electricity Demand Response and Regulation Markets," *IEEE Syst. J.*, vol. 14, no. 3, pp. 3729–3739, 2020, doi: 10.1109/JSYST.2019.2943451.

[41] Q. Guo, T. Guo, Q. Tian, and S. Nojavan, "Optimal robust scheduling of energy-water nexus system using robust optimization technique," *Comput. Chem. Eng.*, vol. 155, p. 107542, 2021, doi: 10.1016/j.compchemeng.2021.107542.

[42] F. M. Al-Fadhli, N. Alhajeri, H. Ettouney, D. Sengupta, M. Holtzapple, and M. M. El-Halwagi, "Simultaneous optimization of power generation and desalination systems: a general approach with applications to Kuwait," *Clean Technol. Environ. Policy*, vol. 24, no. 7, pp. 2129–2141, Sep. 2022, doi: 10.1007/s10098-022-02303-3.

[43] F. M. Al-Fadhli *et al.*, "Optimizing cogeneration and desalination plants by incorporating solar energy," *Desalination*, vol. 549, no. August 2022, p. 116320, 2023, doi: 10.1016/j.desal.2022.116320.

[44] S. Wang, X. Wang, Z. Fu, F. Liu, Y. Xu, and W. Li, "A novel energy-water nexus based CHP operation optimization model under water shortage," *Energy*, vol. 239, 2022, doi: 10.1016/j.energy.2021.121832.

[45] S. Xiao, Q. Guan, W. Zhang, and L. Wu, "Optimal scheduling of the combined power and desalination system," *Energy Reports*, vol. 8, pp. 661–669, 2022, doi: 10.1016/j.egyr.2021.11.253.

[46] J. A. Marmolejo, J. Velasco, and H. J. Selley, "An adaptive random search for short term generation scheduling with network constraints," *PLoS One*, vol. 12, no. 2, pp. 1–17, 2017, doi: 10.1371/journal.pone.0172459.

[47] A. Valero *et al.*, "CGAM problem: Definition and conventional solution," *Energy*, vol. 19, no. 3, pp. 279–286, 1994, doi: 10.1016/0360-5442(94)90112-0.

[48] P. Sharan, T. Neises, and C. Turchi, "Optimal feed flow sequence for multi-effect distillation system integrated with supercritical carbon dioxide Brayton cycle for seawater desalination," *J. Clean. Prod.*, vol. 196, pp. 889–901, 2018, doi: 10.1016/j.jclepro.2018.06.009.

[49] M. Ameri and M. Jorjani, "Performance assessment and multi-objective optimization of an integrated organic Rankine cycle and multi-effect desalination system," *Desalination*, vol. 392, pp. 34–45, 2016, doi: 10.1016/j.desal.2016.04.009.

[50] P. Druetta, P. Aguirre, and S. Mussati, "Minimizing the total cost of multi effect evaporation systems for seawater desalination," *Desalination*, vol. 344, pp. 431–445, 2014, doi: 10.1016/j.desal.2014.04.007.

[51] M. Maheshwari and O. Singh, "Thermo-economic analysis of combined cycle configurations with intercooling and reheating," *Energy*, vol. 205, p. 118049, 2020, doi: 10.1016/j.energy.2020.118049.

[52] A. S. Hanafi, G. M. Mostafa, A. Fathy, and A. Waheed, "Thermo-Economic Analysis of Combined Cycle MED-TVC Desalination System," *Energy Procedia*, vol. 75, pp. 1005–1020, 2015, doi: 10.1016/j.egypro.2015.07.342.

[53] H. El-Dessouky, I. Alatiqi, S. Bingulac, and H. Ettouney, "Steady-state analysis of the multiple effect evaporation desalination process," *Chem. Eng. Technol.*, vol. 21, no. 5, pp. 437–451, 1998, doi: 10.1002/(SICI)1521-4125(199805)21:5<437::AID-CEAT437>3.0.CO;2-D.

[54] P. Sharan, T. Neises, J. D. McTigue, and C. Turchi, "Cogeneration using multi-effect distillation and a solar-powered supercritical carbon dioxide Brayton cycle," *Desalination*, vol. 459, no. October 2018, pp. 20–33, 2019, doi: 10.1016/j.desal.2019.02.007.

[55] F. M. Al-Fadhli *et al.*, "Optimizing cogeneration and desalination plants by incorporating solar energy," *Desalination*, vol. 549, no. November 2022, p. 116320, 2023, doi: 10.1016/j.desal.2022.116320.

[56] A. M. Pietrasanta, S. F. Mussati, P. A. Aguirre, T. Morosuk, and M. C. Mussati, "Optimization of a multi-generation power, desalination, refrigeration and heating system," *Energy*, vol. 238, p. 121737, 2022, doi: 10.1016/j.energy.2021.121737.

[57] P. Roosen, S. Uhlenbruck, and K. Lucas, "Pareto optimization of a combined cycle power system as a decision support tool for trading off investment vs. operating costs," *Int. J. Therm. Sci.*, vol. 42, no. 6, pp. 553–560, 2003, doi: 10.1016/S1290-0729(03)00021-8.

[58] UAE Ministry of Energy, "UAE STATE OF ENERGY REPORT," 2015. [Online]. Available: https://u.ae/en/information-and-services/environment-and-energy/water-and-energy/electricity, Accessed: April 10, 2023.

[59] SCAD, "Energy and Water Statistics 2017," 2017. [Online]. Available: https://www.scad.gov.ae/Release Documents/Energy and Water 2017 EN.pdf.

[60] Andreas, A.; Stoffel, T.; (2006). Nevada Power: Clark Station; Las Vegas, Nevada (Data); NREL Report No. DA-5500-56508. http://dx.doi.org/10.5439/1052547, Accessed: 23 March, 2023.

Vita

Mennatalla Ahmed Elbalki was born in 1999, in Cairo, Egypt. She received her primary and secondary education in Abu Dubai, UAE. She received her B.Sc. in Electrical Engineering from Abu Dhabi University in 2021. During her bachelor's study, she co-authored one article published in a reputable journal.

Soon after graduating, she joined the Electrical Engineering master's program at the American University of Sharjah as a graduate research and teaching assistant. Her research interests are optimization in electrical engineering, renewable energy, water sustainability, and smart grids.